

FINAL REPORT

of the research project #K101854 (and the linked #101897), entitled by „AEROBIC SELECTIVE OXIDATION ON GOLD-CONTAINING BIMETALLIC CATALYSTS”

supported by the Hungarian Science and Research Fund and the National Research, Development and Innovation Office

The project started in 2012, when it was already well reported that gold catalysts are very promising for selective oxidation reactions performed by pure O₂ or air as eco-friendly^{1,2,3} oxidant. Moreover there were already many examples published on bimetallic Au-Pd, Au-Pt catalysts and also several on Au-Ag^{4,5} and Au-Cu⁶ with improved performance compared to monometallic counterparts. We aimed at studying bimetallic gold catalysts with four different second metals (Ag, Cu, Ru and Ir) to investigate the structure and catalytic performance relationship, with special attention to the interaction of the two metals in the catalysts. For model selective oxidation catalytic test reactions glucose and benzyl alcohol substrates, and in case of Au-Ag/Al₂O₃ catalysts, in collaboration with Italian researchers in the frame of a CNR-MTA bilateral research co-operation, also glycerol were applied.

For this purpose catalysts were prepared for all four bimetallic systems by the same method, by immobilisation of preformed bimetallic nanoparticles (NPs) from bimetallic aqueous sols on alumina and in case of Au-Ag and Au-Cu systems also on silica support. This preparation method was chosen for providing intimate contact of the two metals, by formation of truly bimetallic particles. The details of Au-Ag/SiO₂ catalysts preparation was reported in ref. ⁷. In this case to avoid the AgCl precipitation the precursor ions were reduced subsequently (first AgNO₃, then HAuCl₄ on the Ag NPs: Au->Ag) by NaBH₄ in presence of polyvinyl alcohol stabilising agent. Samples with different Au/Ag atomic ratio were produced. The Au-Cu NPs were fabricated by the same reducing and stabilizing agents and reagent concentrations performing three different order of reduction, co-reduction (Au&Cu) and consecutive reductions (Cu->Au and Au->Cu) of the precursor ions to produce particles of different structure. In case of Au-Ru and Au-Ir bimetallic sols co-reduction was applied. For the Au-Cu, Au-Ru and Au-Ir systems Au/M=1/1 atomic ratio was intended. The metal NPs of sols were easily and completely adsorbed on the supports for providing typically 0.1, in some cases 0.2 mmol/g_{cat} metal concentration, on alumina without using any additive, on silica with addition of poly-diallyl-dimethyl-ammonium chloride (PDDA) to provide the proper surface charge for complete adsorption. In the CNR-MTA collaboration Au-Ag/Al₂O₃ systems were formed also by the solvated metal atom dispersion (SMAD) deposition method and compared with the sol derived catalysts. The corresponding monometallic samples were prepared for all four bimetallic systems. The supported catalysts were studied in catalysis typically after calcination treatment (400°C/air/1h or 30min) applied for removal of organic residues from the active sites and also after subsequent mild reduction (350°C or 400°C/H₂/30min) to provide the metallic state, and in some cases also after further reduction (500°C/H₂/2h) to allow some restructuring (rather alloying) of metal NPs.

The catalyst structures were investigated at different stages of the preparation and after the pretreatments applied. The metal loading of the samples was checked by prompt-γ activation analysis. The modification of the localised surface plasmon resonance (SPR) of gold on the effect of the second metal and pretreatments was investigated by UV-vis spectroscopy (in transmission for sols and diffuse reflectance for supported samples). Transmission electron microscopy (TEM) was applied for particle size measurements, high resolution (HR) TEM for determination of the lattice parameters in the different particles. By scanning transmission electron microscopy (STEM) measurements in combination with energy dispersive x-ray spectroscopy (EDS) in the frame of ESTEEM-2 Transnational Access at Institute for Electron Microscopy and Nanoanalysis, Graz University of Technology and in the CNR-MTA co-operation project at ISTM-CNR for the Au/M atomic ratio was measured in single particles of the sols and selected supported samples. X-ray diffraction (XRD) was also measured, however, in most of the cases very weak reflections of the active components were observed due to the low concentration and small crystallite sizes. ¹⁹⁷Au Mössbauer spectroscopy measurements were performed on the as prepared alumina supported Au&Cu and Cu->Au samples using eight times higher metal loading to increase the signal intensity for good quality Mössbauer spectra. Temperature programmed reduction measurements were performed for studying the reducibility of the second metal in the bimetallic catalysts in comparison with that of the corresponding monometallic ones. X-ray photoelectron spectroscopy gave information about the surface layer composition of the catalysts and the oxidation state of the components. The top surface composition of the catalysts was traced by CO adsorption measurements taking into account the limitations of this method, namely, on the contrary Ru and Ir strongly adsorbing CO, on gold, silver and copper sites CO adsorption is very weak and reversible. Moreover, only special Au sites with low coordination number can adsorb CO at room temperature; metallic Ag cannot adsorb CO (at low CO partial pressure), only Ag⁺ sites; Cu²⁺ does not adsorb CO, only Cu⁺ and even weaker Cu⁰. CO adsorbed was studied by diffuse reflectance Fourier transformed IR (DRIFT) spectroscopy under 10 mbar CO, by that the adsorption sites could be differentiated by the frequency and stability of CO stretching bands. On the other side the amount of CO adsorbed at -20°C in equilibrium with 10 mbar CO was measured by QMS from the loss of CO from the 1%CO+1%Kr/Ar flow contacting with the catalyst. The CO uptake was calculated from the concentration difference between CO and the

not adsorbing reference Kr in the effluent gas flow after switching 1%CO+1%Kr/Ar on the catalyst, and from the desorption after changing back to inert Ar flow and following temperature programmed desorption.

The catalytic tests were carried out in liquid phase under intense stirring. The reaction conditions were the following. Benzyl alcohol (BnOH) oxidation: 30 mL 1M or 0.1M BnOH in toluene solution in base free conditions or with equimolar K₂CO₃ addition, 80°C, 1 bar O₂ bubbling. Glucose (Glu) oxidation: 30 mL 0.1 M aqueous Glu solution, 35°C, 1 bar O₂ bubbling, pH=9 provided by 0.1M carbonate-bicarbonate (volume ratio: 2:3) buffer solution. Glycerol (Gly) oxidation: 10 mL 0.3M aqueous Gly solution with 4 eq. NaOH addition, 50°C, 3 bar O₂. Substrate/metal ratio varied between 4000-750. The selectivity of gluconic acid in Glu oxidation was 100% for all catalysts, in BnOH oxidation beside benzaldehyde the only by-product detected was benzyl-benzoate with selectivity lower than 12%. In Gly oxidation many products were observed, their selectivity changed significantly on the different catalysts.

In the following the most important results on the four different bimetallic systems are reviewed separately.

Au-Ag bimetallic systems

Au-Ag/SiO₂

The results of structural and catalytic investigation of Au→Ag/SiO₂ catalyst systems were published in ref. 7,8. Bimetallic samples of various Ag/Au ratio contained particles of 3-5 nm mean diameters stable in the calcination and mild reduction treatments (Table 1.). The single SPR band in the **UV-vis spectra** of both the sol and supported samples shifted from the one characteristic of monometallic gold towards the one of monometallic silver in calcined (Fig. 1.) and reduced state indicated the presence of alloyed particles. The wavelength of SPR bands changed roughly linearly with the Au/(Au+Ag) bulk atomic ratio, suggesting that the alloy composition was close to the bulk Au/Ag value.

Table 1. Metal content and particle sizes of the catalysts determined by PGAA and TEM, respectively.

Catalysts	Ag/Au atomic ratio	Metal content		Mean particle size (nm)		
		Ag (mmol/g cat.)	Au (mmol/g cat.)	after calcination	after reduction	after reaction
Au/SiO ₂	0/100	0	0.190	4.8 ± 2.4	4.0 ± 2.0	-
10Ag90Au/SiO ₂	13/87	0.014	0.093	3.5 ± 2.3	3.1 ± 1.6	3.5 ± 2.0
20Ag80Au/SiO ₂	23/78	0.025	0.085	2.9 ± 1.2	3.5 ± 1.7	-
33Ag67Au/SiO ₂	33/67	0.033	0.067	3.4 ± 2.5	3.3 ± 1.2	-
50Ag50Au/SiO ₂	51/49	0.049	0.051	5.2 ± 2.2	-	-
Ag/SiO ₂	100/0	0.092	0	4.8 ± 3.5	4.9 ± 3.6	-

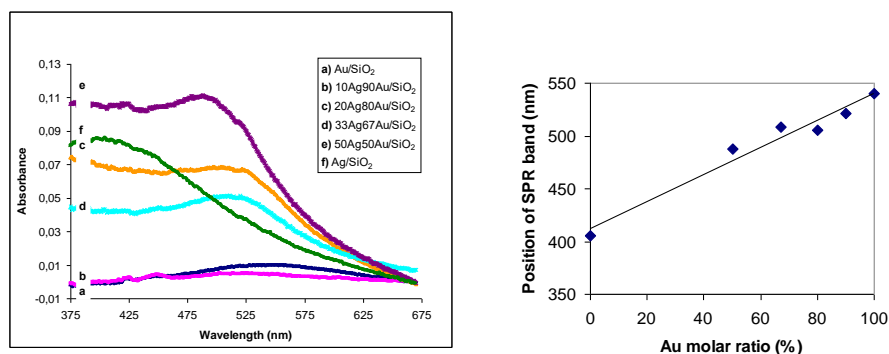


Fig 1. UV-Visible spectra (left) and UV-Vis absorption band maximum of Ag→Au/SiO₂ catalysts versus Au molar fraction (right) after calcination in air at 400°C

Table 2. XPS data of Au→Ag/SiO₂ catalysts

Catalysts	Au binding energy (eV)		Ag binding energy (eV)		Ag/Au atomic ratio		
	calcination	reduction	calcination	reduction	bulk	surface	
						calcination	reduction
Pretreatments							
Au/SiO ₂	83.0	83.0	-	-	-	-	-
10Ag90Au/SiO ₂	82.9	82.8	367.0	366.8	0.15	0.18	0.17
20Ag80Au/SiO ₂	82.9	82.8	367.5	367.3	0.29	0.34	0.28
33Ag67Au/SiO ₂	82.9	83.2	367.0	367.1	0.49	1.14	1.00
50Ag50Au/SiO ₂	82.9	83.1	367.4	367.3	0.95	1.17	1.17
Ag/SiO ₂	-	-	368.6	367.2	-	-	-

XPS did not show significant shift of Au 4f binding energies (BEs) of Au/SiO₂ on the effect of Ag second metal and did not change on calcination and reduction treatment (see Table 2.). The Ag 3d bands appeared at higher BEs in the calcined monometallic Ag/SiO₂, than in the bimetallic ones, and while the reduction caused no significant changes in case of the latter's, the BEs of Ag 3d of monometallic Ag decreased to about the same value measured for the bimetallic catalysts. The oxidation of Ag during calcination was supposed in Ag/SiO₂, which could be then reduced to metallic Ag again (on the contrary that the shift of Ag 3d bands were opposite to that reported in many papers), while in bimetallic samples the metallic state of Ag was retained in calcination, possibly due to the alloying with gold. The surface Ag/Au ratio was higher, than the bulk value showing some enrichment of Ag on the surface, which slightly decreased after reduction.

The bimetallic Au→Ag/SiO₂ with Ag/Au=33/67 or lower atomic ratio had large synergetic effect (the largest the catalyst of Ag/Au=23/77) in both calcined and reduced state in both **glucose and base free benzyl alcohol selective oxidation** based on the initial reaction rates as shown on Fig. 2 a and b. However, in the BnOH oxidation the catalysts quickly deactivated, below 5% conversion the reaction slowed down, possibly due to the poisoning by the trace amount of benzoic acid side product. The sample of Ag/Au=50/50 and the monometallic Ag/SiO₂ were not active under the applied reaction conditions. In case of Glu oxidation the samples of Ag/Au=23/77 and 33/67 were slightly more active after reduction, than after calcination, which could be partly in relation with the lower Ag/Au surface atomic ratio in the former state. In BnOH oxidation the reduced samples were much more active than the calcined ones that could not be due to only the influence of the surface concentration changes, because it was valid for the monometallic Au/SiO₂, as well. Maybe also the silica surface changed in the pre-treatments, and the reaction media (basic aqueous and base free toluene solution) could play a role in the stronger pretreatment effect in BnOH oxidation.

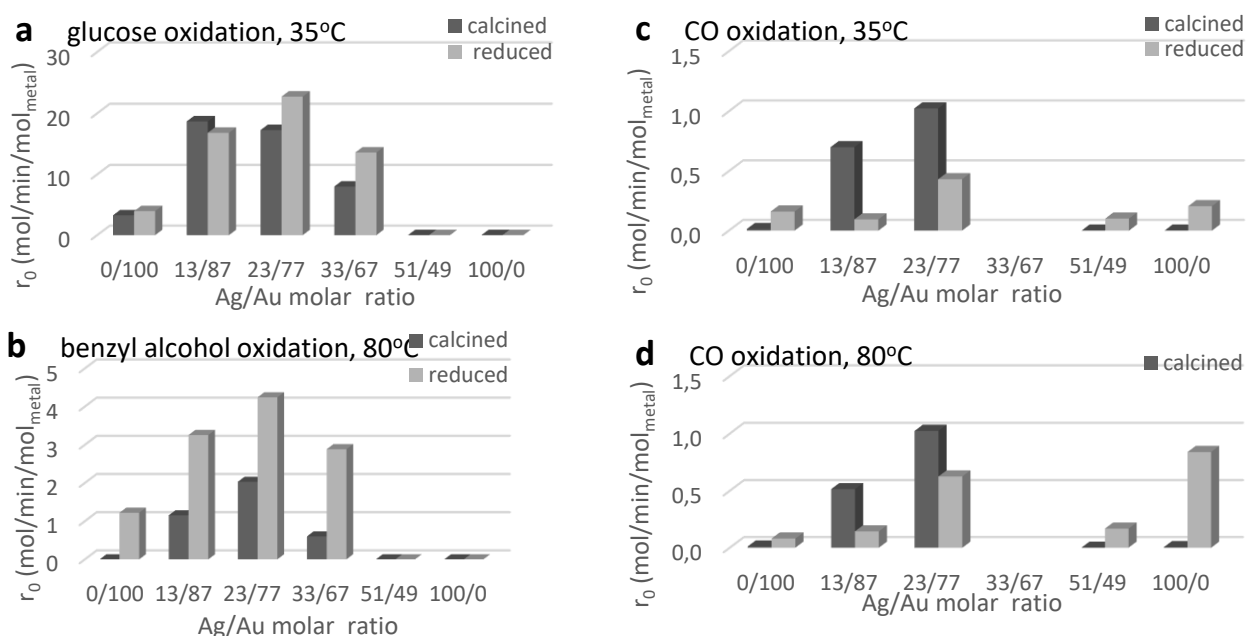


Fig. 2 Initial reaction rates of the various Au→Ag/SiO₂ in glucose (0.1 M Glu in aqueous solution), benzyl alcohol (1.0 M BnOH in toluene solution) and CO oxidation (1 bar 0.5% CO+10% O₂ in He, 40 mg catalyst)

Also gas phase temperature programmed **CO oxidation reaction** (Fig. 2 c and d) were carried out to characterize the catalyst surface. Strong synergetic activity increase was observed on the calcined samples at lower Ag/Au ratio, where the monometallic analogous were inactive, while in reduced form the bimetallic catalysts became less active, the monometallic Au/SiO₂ and Ag/SiO₂ became active, the synergetic effect decreased. The active sites of the selective oxidation reaction and CO oxidation must have been different.

The most active 23Ag77Au/SiO₂ and the monometallic Au/SiO₂ were measured in benzyl alcohol oxidation also with base addition (equimolar K₂CO₃), which eliminated the benzoic acid poisoning. The results are presented on Fig. 10 c and discussed later. Benzoic acid addition (BnOH/benzoic acid=1000:1) to base free reaction mixture blocked the reaction, while in presence of equimolar K₂CO₃, the 10 times higher amount benzoic acid addition did not affect the reaction, the BnOH conversion could be completed.

Au-Ag/Al₂O₃

The most active Au/Ag=80/20 composition (designated from here as Au4Ag1) observed among the silica supported Au→Ag catalysts, and also the Au/Ag=1/1 (Au1Ag1) composition were prepared on alumina by the same preparation technique (SOL) as used for the silica supported systems, and also by SMAD deposition method. The particle sizes in

these catalysts after different treatments are summarised in Table 3. The particles of sol derived samples were smaller than earlier in the silica supported samples. The same sol preparation resulted smaller particles, which could be the reason of using different quality ultrapure water. The mean diameter of Au containing particles in the different SOL samples varied between 1.9 and 2.4 nm, while the SMAD preparation resulted in larger particles with average diameter between 3.5-4.4 nm. The Ag particles produced by both methods were larger with wide size distribution, however the smaller ones was difficult to recognise on TEM images on the crystalline alumina particles. The particle sizes in SOL samples did not change much in the different treatments except in monometallic Ag/Al₂O₃, in SMAD ones some sintering, especially in bimetallic samples was observed. About 15-15 particles were measured by HR-EDS in the bimetallic catalysts, and all of them were bimetallic, the mean Au/Ag atomic ratio close to the bulk value in case of Au₄Ag₁/Al₂O₃ samples, and somewhat higher than that in SOL Au₁Ag₁/Al₂O₃.

Table 3 Metal loading, mean particle sizes and average Au concentration in bimetallic particles

		SOL					SMAD			
		Au/ Al ₂ O ₃	Au*/ Al ₂ O ₃	Au ₄ Ag ₁ / Al ₂ O ₃	Au ₁ Ag ₁ / Al ₂ O ₃	Ag/ Al ₂ O ₃	Au/ Al ₂ O ₃	Au ₄ Ag ₁ / Al ₂ O ₃	Au ₁ Ag ₁ / Al ₂ O ₃	Ag/ Al ₂ O ₃
Metal loading	Au wt%/Ag wt%	1.8 / 0	1.8/0	2.9/0.5	1.9/0.9	0/2.0	1.8/0	2.9/0.4	1.8/1.0	0/1.0
Mean particle diameter (nm)	as prepared	2.2±0.7	1.9±0.7	2.4±0.7	1.9±0.5	7.5±5.1	3.8±1.5	3.5±2.2	4.4±2.2	8-50
	calc. 400°C/air/0.5h	1.9±0.5	1.9±0.5	2.8±0.6	1.9±0.6	17.1±10.9	5.2±2.4	7.8±2.7		6-35
	red. 400°C/H₂/2h	2.1±0.5		2.8±0.9		27.3±17	4.5±2.6			
Au concentration in single particles, at %	as prep.			77±13				82±8		
	calc.			83±7	65			87±7		

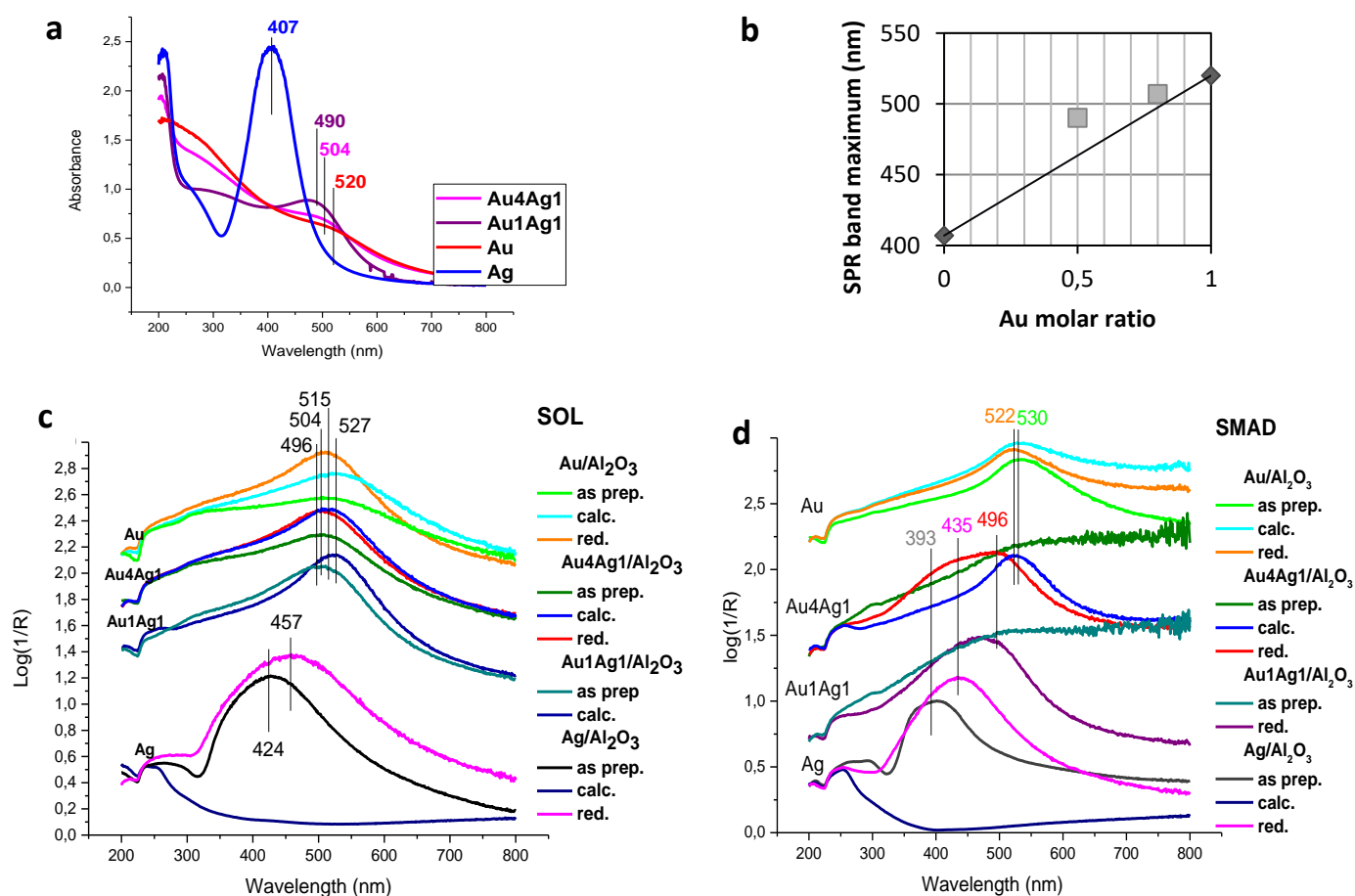


Fig. 3 UV-vis spectra of sols (a), relation between the wavelength of SPR band maxima and the Au molar ratio (b), UV-vis spectra of the alumina supported SOL (c) and SMAD (d) samples

The **UV-vis** spectra of bimetallic sols showed single SPR bands characteristic of alloyed phases with slightly smaller shift compared to the monometallic Au sol towards the band of Ag, than expected for the nominal Au/Ag ratio as visible on Fig. 3 a,b. In the spectra of as prepared supported SOL samples similar SPR band positions could be observed as in sols (Fig.3 c). After calcination the bands red shifted in all the samples, except Ag/Al₂O₃ where the SPR band of Ag disappeared likely due to the oxidation of Ag. The difference between the wavelength of SPR band of Au4Ag1/Al₂O₃ and Au/Al₂O₃ further increased, while that in case of Au1Ag1/Al₂O₃ decreased, as if in the latter catalyst the Au/Ag alloy composition would have increased. On reduction the SPR band of Au4Ag1/Al₂O₃ and Au/Al₂O₃ moved back to the same position as were in the as prepared samples, while in case of Ag/Al₂O₃ appeared again the SPR band of metallic Ag NPs, but at higher wavelength as was in as prepared state. The monometallic SMAD samples had similar spectra as the corresponding sol ones, except that Ag SPR band appeared at lower wavelength (Fig. 3d). The bimetallic SMAD catalysts in as prepared state did not present clear bands, on the high wavelength side they had high extinction. After calcination the SPR band of Au4Ag1/Al₂O₃ was hardly shifted compared to that of Au/Al₂O₃, and after following reduction a wide, two component band appeared at lower wavelength suggesting the co-presence of AuAg alloy phase and also monometallic Ag. The reduced Au1Ag1/Al₂O₃ presented similar overlapping bands, but slightly blue shifted likely indicating alloy component of higher Ag concentration.

Based on UV-vis spectroscopy results it is suggested that AuAg alloy phase was present in bimetallic sols and in as prepared SOL samples. After calcination some segregation of Ag on the surface of alloy particles with increased Au/Ag alloy composition (rather in Au1Ag1/Al₂O₃ than in Au4Ag1/Al₂O₃), after following reduction reverse changes happened. In the SMAD samples the Ag segregation in calcination was stronger, after following reduction beside alloy phase monometallic Ag phase appeared likely on the surface of bimetallic particles or also separately.

CO₂ evolution curves recorded in **TPO** of the different as prepared samples are shown in Fig. 4. CO₂ originated from oxidation of organic contamination. This was expected in case of the SOL samples (stabilizing agent residues), but even from SMAD samples evolved CO₂ in lower amount up to 400°C. The one hour calcination of the as prepared catalysts at 400°C could remove the organic contamination from the surface of metal particles in SOL catalysts, as the band maximum of TPO curve was below 400°C, but on Au-containing SMAD catalysts it was not sure that the surface of active sites was fully cleaned, since the TPO band maximum was not reached up to 400°C.

In **TPR** (see Fig. 5) of calcined SOL Au/Al₂O₃ and SOL Au4Ag1/Al₂O₃ no significant H₂ uptake was measured indicating that Au and Ag dominantly retained their metallic state during calcination. Both calcined SOL and SMAD monometallic Ag/Al₂O₃ and SMAD Au4Ag1/Al₂O₃ consumed large amount H₂, 45%, 100% and 100%, respectively, of the theoretical consumption of reduction all silver from Ag₂O to Ag⁰.

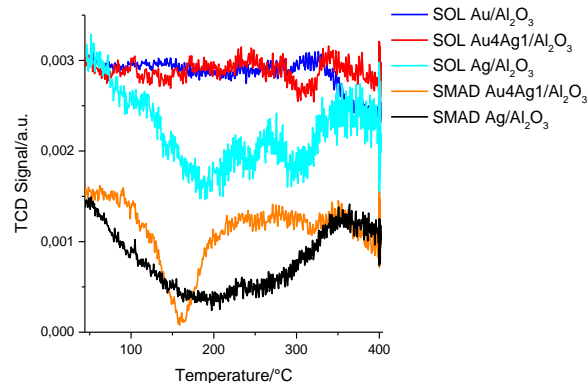
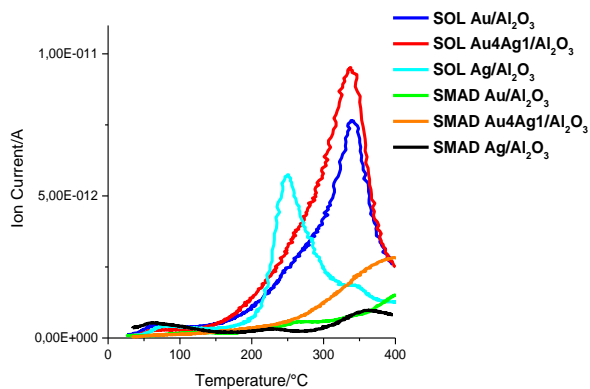


Fig. 4 CO₂ evolution in TPO of the as prepared samples. **Fig. 5** TPR of the different calcined samples. (The curves are normalized for 100 mg catalyst amount.)

XPS measurements were performed on SOL and SMAD Au4Ag1/Al₂O₃ and the monometallic SOL catalysts in as prepared state, after an in situ calcination (400°C/air/30min), a subsequent reduction (400°C/H₂/2h) and a second calcination (400°C/air/30min) treatment. As an illustration the spectra recorded on SMAD Au4Ag1/Al₂O₃ can be seen on Fig. 6. The changes of binding energies (BE) of Au 4f_{7/2} and Ag 3d_{5/2}, and the Ag/Al, Au/Al and Au/Ag surface atomic ratios in the different samples after different treatments are visualized on Fig. 7. Gold was in metallic state in all the samples, however the Au 4f_{7/2} BE of SOL Au4Ag1/Al₂O₃ was about 0.5 eV higher than that of SMAD Au4Ag1/Al₂O₃ and SOL Au/Al₂O₃, maybe because of stronger interaction between Au and Ag than in SMAD catalyst. The Au 4f_{7/2} BEs does not change significantly on the effect of the oxidative and reductive treatments. Similar Ag 3d_{5/2} BE was measured in the as prepared and in the calcined Ag/Al₂O₃, which decreased by about 0.8 eV after reduction, then could be restored by a second calcination. The lower BE was assigned to metallic Ag, while the higher to oxidised Ag, supposedly Ag₂O. In SOL Au4Ag1/Al₂O₃ BE of Ag 3d_{5/2} hardly changed on the effect of pretreatments and its value was about the same as in case

of reduced SOL Ag/Al₂O₃, so dominantly metallic state of Ag was maintained in all the treatments applied, so Ag must have been in alloy phase that could stabilize metallic Ag. The SMAD Au₄Ag₁/Al₂O₃ behaved more similar to monometallic Ag/Al₂O₃, but in as prepared state Ag was rather metallic in the bimetallic sample, while oxidised in the monometallic sample. These findings were quite in accordance with the TPR and UV-vis results.

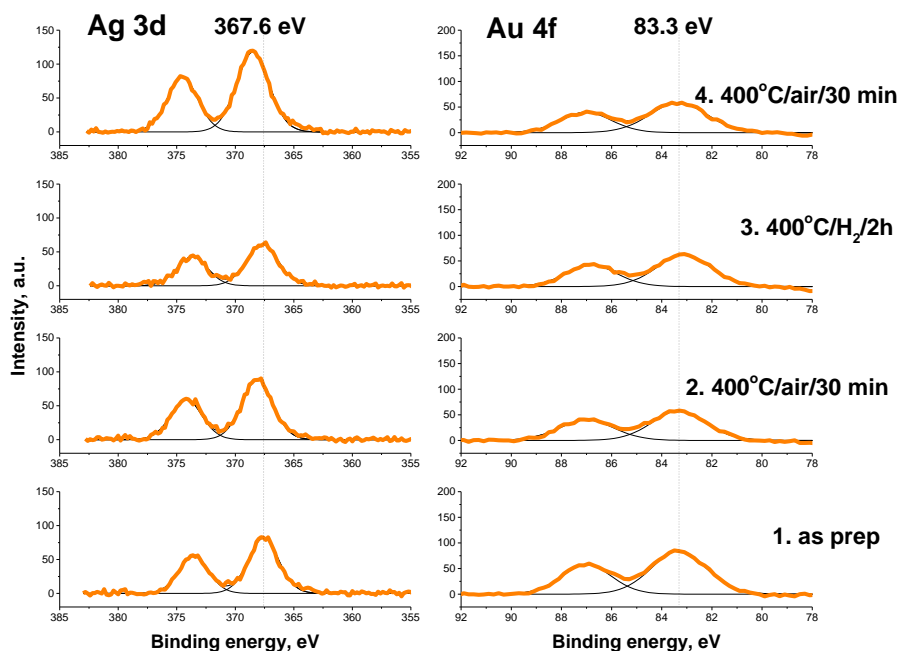


Fig. 6 XP spectra of SMAD Au₄Ag₁/Al₂O₃ (0.2 mmol metal/g_{cat}) after various in situ pretreatments

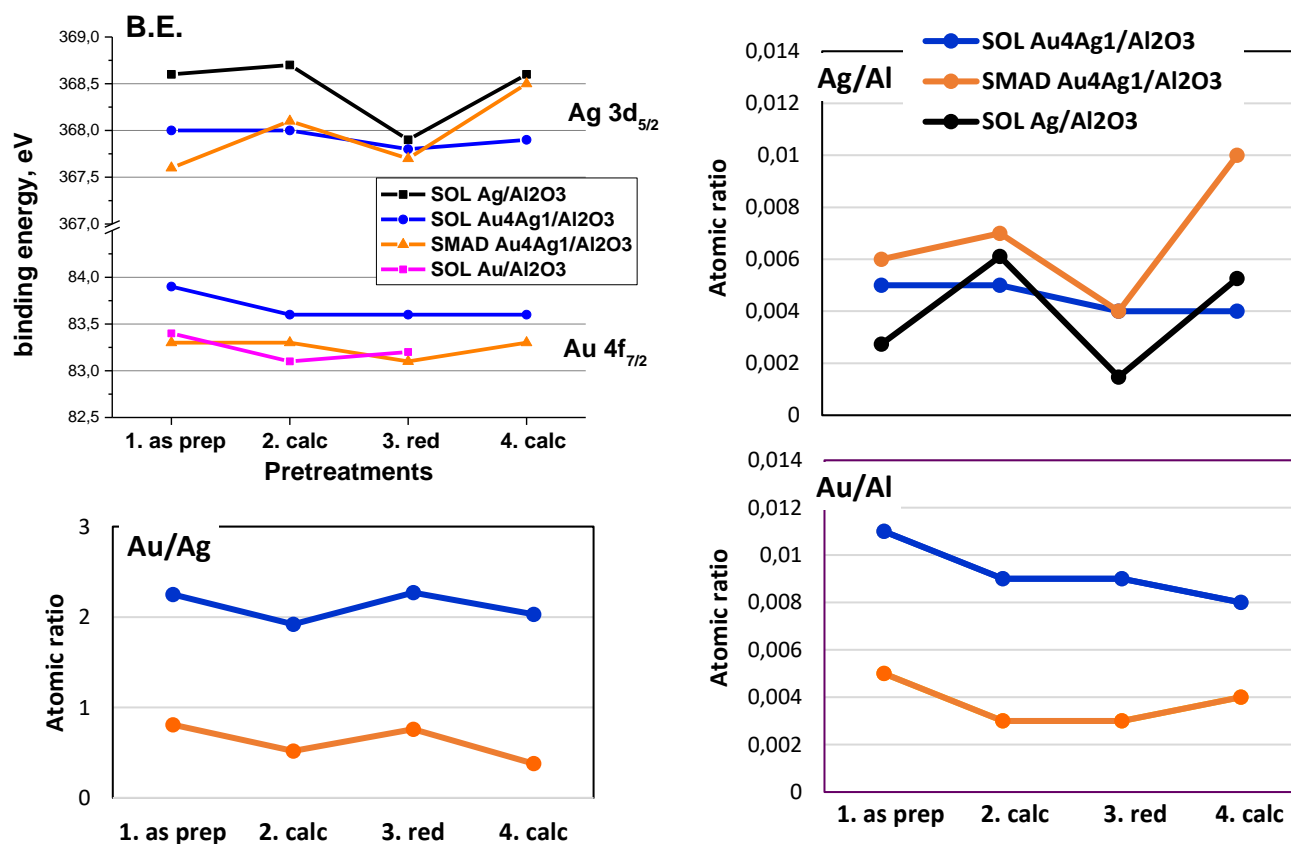


Fig. 7 Changes of Ag 3d_{5/2} and Au 4f_{7/2} BEs and Ag/Al, Au/Al (related to the same 0.16 mmol/g_{cat} Au and 0.04 mmol/g_{cat} Ag loading), Au/Ag surface atomic ratio in XP spectra of different samples after various in situ treatments.

In Ag/Al₂O₃ the Ag/Al surface atomic ratio changed drastically and reversibly in the calcination-reduction-calcination treatment series. In calcination it increased, after reduction decreased, what could be explained by spreading Ag-oxide over alumina support due to some interaction, and sintering of metallic Ag. In SOL Au₄Ag₁/Al₂O₃ Ag/Al atomic ratio was quite constant during the different treatments, Ag likely was well localised in AuAg alloy. The SMAD Au₄Ag₁/Al₂O₃ was more similar to monometallic Ag/Al₂O₃, so silver was more mobile in this catalyst, part of them could be separated from Au. The Ag/Al ratio (normalised to the same Ag loading, 0.4 wt %) was the highest in SMAD Au₄Ag₁/Al₂O₃ (Ag was more enriched on the surface than in corresponding SOL sample), and the Au/Al ratio was much lower in SMAD bimetallic catalyst, than in SOL one, partly because of larger particle size, partly because of possible higher enrichment of Ag on the bimetallic particle surface. Au/Ag was more than two times higher in the SOL than in SMAD sample, and in both cases showed some fluctuation, small decrease in calcined, small increase in reduced state.

CO adsorption studies were performed for characterisation the top surface of the different catalysts. The DRIFT spectra of the samples after various in situ pretreatments in presence of 10 mbar CO are presented on Fig. 8. After purging with inert gas the bands of CO adsorbed disappeared quickly. In as prepared state only very weak CO bands formed on SOL samples (not shown) possibly because of the adsorption sites were occupied by the organic residues and other weakly bonding adsorbed molecules as water. In the spectra of ex situ calcined monometallic SOL Au/Al₂O₃ sample strong CO stretching band appeared at 2106 cm⁻¹ characteristic of linearly adsorbed CO on metallic Au atoms of low coordination number. After following short in situ calcination at 400°C/5min, when the catalyst was cooled in the synthetic air, two overlapping bands, a stronger at 2111 cm⁻¹ and a weaker at about 2124 cm⁻¹ evolved, while after following reduction treatment at 350°C/30min and a subsequent one at 500°C/30min only one single band at 2106 cm⁻¹ was visible with the same intensity. A subsequent calcination resulted again the blue shifted CO bands, but at even higher frequency. The higher frequency bands are typically assigned to CO adsorbed on partially positively charged Au^{δ+} likely formed by interaction with adsorbed O₂. These bands shifted back to about 2106 cm⁻¹, when the catalyst was purged with inert gas before CO adsorption or during longer exposure to 1%CO/Ar mixture (these spectra not shown), presumably because of desorption of oxygen. On calcined SOL Ag/Al₂O₃ the band at 2164 cm⁻¹ was characteristic of CO adsorbed on Ag⁺. The band intensity of CO adsorbed on Ag⁺ was smaller, than that on Au in SOL Au/Al₂O₃. By reduction at 350°C this band almost disappeared indicating the almost complete reduction of silver (at 10 mbar CO partial pressure at room temperature metallic Ag does not adsorb CO). On the bimetallic SOL Au₄Ag₁/Al₂O₃ catalyst the bands characteristic of CO adsorbed on both Au⁰ and Ag⁺ appeared with lower intensity, but at the same frequencies as on the monometallic Au and Ag samples, respectively. However, the band assigned to CO on Au^{δ+} shifted to significantly higher frequency indicating larger partial positive charge on Au supposedly due to stronger interaction with oxygen in presence of Ag⁺. On the SOL Au₁Ag₁/Al₂O₃ no CO adsorbed on Au sites were visible in the spectrum after calcination beside that of adsorbed on Ag⁺. After reduction at 350°C very weak bands of CO on Au⁰ appeared, which increased only a bit after reduction at 500°C, showing low concentration of accessible Au sites in this sample.

The CO adsorption gave much different results on the SMAD samples. First of all the SMAD Au₄Ag₁/Al₂O₃ did not show adsorbed CO band, not in as prepared, nor in calcined and reduced states, possibly because of contamination blocking the adsorption sites. Using higher temperature calcination (500°C) these contamination could be removed (at least partially), and a band at 2174 cm⁻¹ appeared due to CO adsorbed on Ag⁺, while no clear sign of CO on Au could be observed, likely silver enriched on the surface of bimetallic particles. On SMAD Au₁Ag₁/Al₂O₃ Ag⁺ sites could be detected even after the normal calcination treatment, and a weak band of CO on Au appeared after reduction. On the SMAD Au/Al₂O₃ much lower band intensities were observed than on SOL one, and the band positions were also different, in calcined state at 2156 cm⁻¹, in reduced state at 2115 cm⁻¹, which both were blue shifted compared to the SOL case suggesting somewhat different Au sites, likely lower CO coverage. On Ag/Al₂O₃ the band position was about the same as on the corresponding SOL catalyst, with intensity of about 30% of that measured on the SOL analogue.

The comparison of the quantity of adsorbed CO based on its DRIFT spectra is somewhat uncertain, because of the not fully controlled reflection conditions of the sample powders and the possibly different molar extinction coefficients of CO adsorbed on different sites. That is why **CO-TPD measurements** followed by QMS were performed after CO adsorption at -20°C (-20°C/1%CO-Ar/10min then -20°C/Ar/10 min) to estimate the amount of CO adsorbed. The CO and CO₂ evolution curves in TPD of the calcined and subsequently reduced monometallic SOL samples and bimetallic ones prepared by both SOL and SMAD methods are collected in Fig. 9. At the applied conditions the pure alumina support itself showed negligible CO desorption in TPD (shown as on Fig. 19). CO₂ evolution accompanied the CO one only in the case of the calcined SOL samples rather the Au-containing ones. A tentative explanation for this, that oxygen adsorbed present on the surface after calcination (with cooling down in the O₂ containing gas mixture) interacting with adsorbed CO could form CO₂ that was retained on the alumina support up to about 180-200°C likely in form of carbonates. The largest amount of CO desorbed from the calcined Ag/Al₂O₃, while from its reduced form no CO desorbed, what meant in accordance with the expectations and DRIFT measurements that no CO was adsorbed. Both calcined and reduced SOL Au/Al₂O₃ presented CO desorption, but in much lower amount than the calcined Ag/Al₂O₃. The desorption band was somewhat higher on the calcined, than on the reduced Au/Al₂O₃.

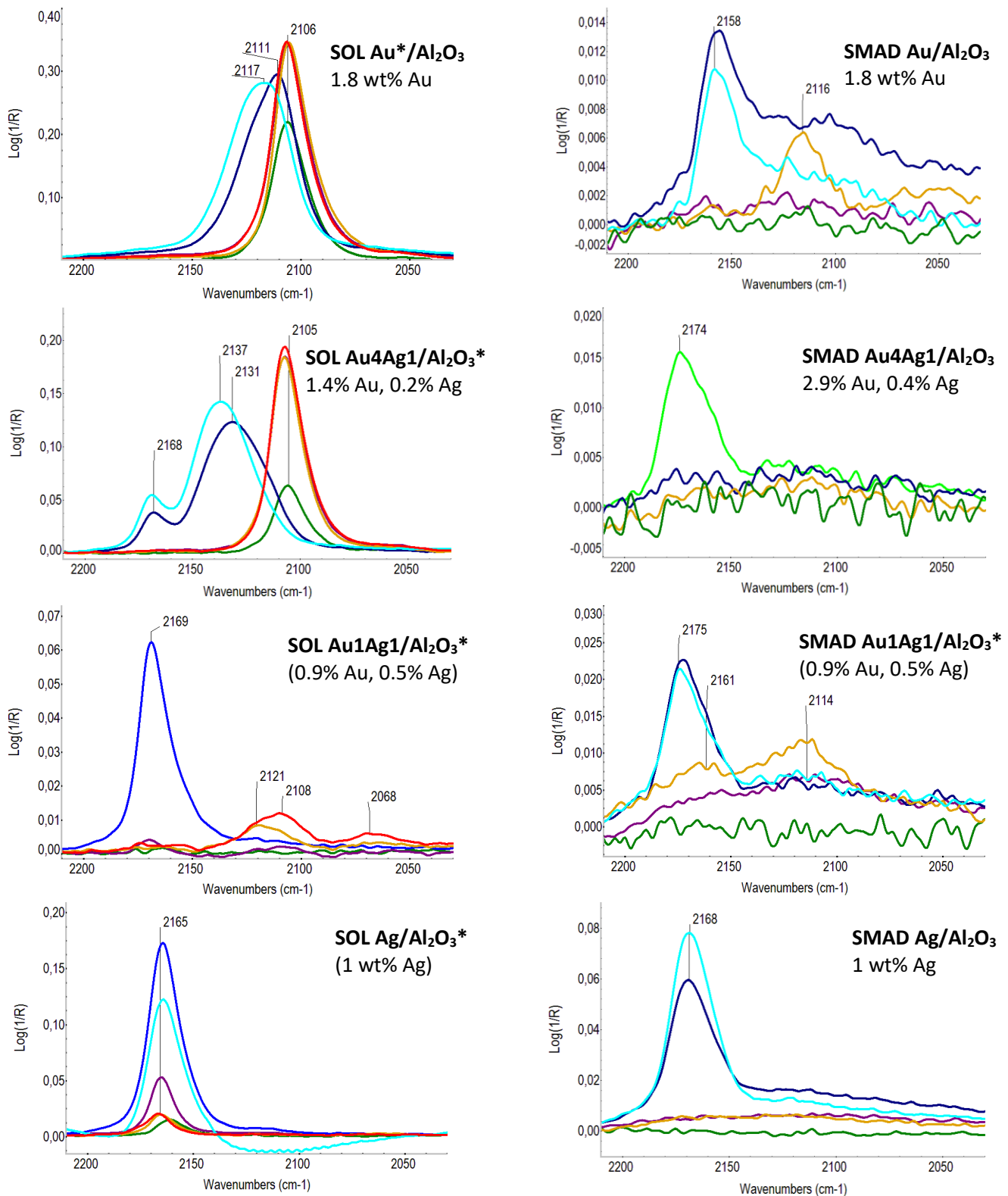


Fig. 8 DRIFT spectra of CO adsorbed at room temperature (in presence of 1% CO/Ar) on different SOL (on the left side) and SMAD (on the right side) samples after different treatments. (Spectrum of gas phase CO was subtracted.)

SOL calcined *ex situ* (air/400°C/1h), **SMAD** as prepared; **Ar/400°C**; **Calc.** (air/400°C, cooling in air); **Red.** (H₂/350°C); **Red.**(H₂/500°C); **Reoxidation** (air/400°C, SOL Ag: 200°C, cooling in air); **Reoxidation** (air/500°C, cooling in air)

On bimetallic samples the CO evolved from calcined samples could be attributed to both Au and Ag⁺, while from reduced sample only to Au. In the reduced state on SMAD Au₄Ag₁/Al₂O₃ no, while on SOL analogue similar amount of Au sites adsorbing CO was observed than on Au/Al₂O₃, that was, however, about 65% of that on Au/Al₂O₃ related to the same Au content. On both calcined bimetallic samples the larger CO desorption bands than on corresponding reduced ones indicated that Ag⁺ was available on the surface, but less than on the monometallic Ag/Al₂O₃. The amount of CO

desorbed during the CO-TPD of different samples normalised to 1 mmol metal (Au+Ag) content are presented in Table 4.

On SMAD Au4Ag1/Al₂O₃ after additional calcination up to 600°C accompanied by remarkable CO₂ formation, largely increased CO adsorption (as deduced from CO desorption) took place (not shown), that confirmed the blocking effect of organic residues remained after 400°C calcination. The same treatment of SOL Au/Al₂O₃, during that hardly any additional CO₂ formation was observed, significantly decreased the CO adsorption as a result of possible sintering of Au (these result are not shown here).

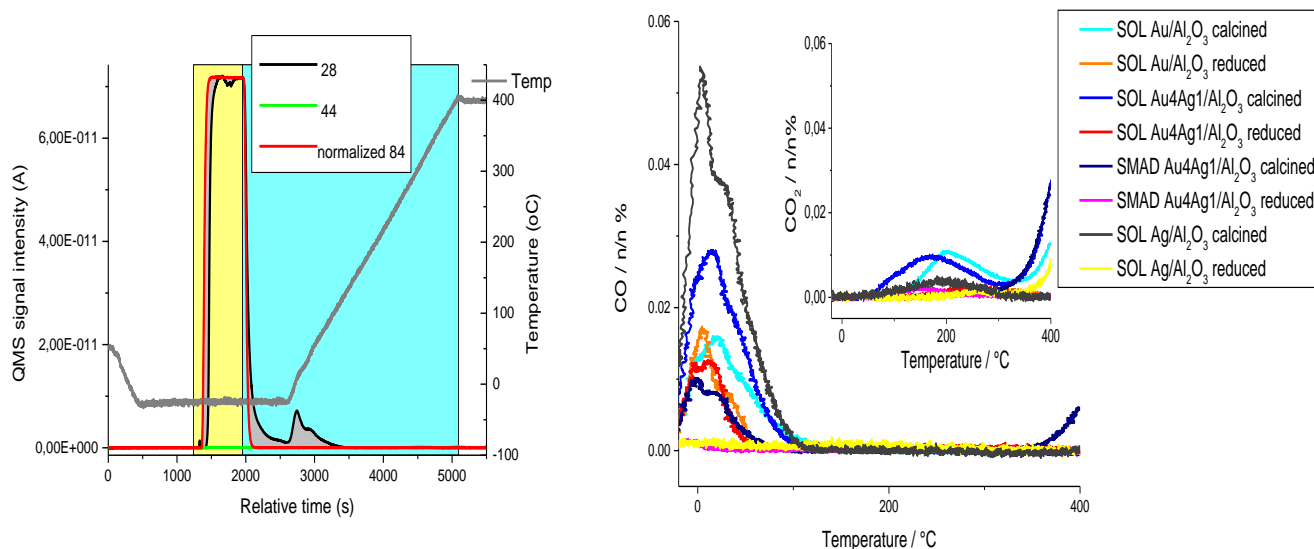


Fig. 9 TPD of CO adsorbed at -20°C on different samples calcined (400°C/10%O₂-He/30 min followed by cooling in the same gas mixture) and subsequently reduced (400°C/10%H₂-Ar/2h). In the inset the CO₂ evolution during CO-TPD is shown. The TPD curves were normalised to 100 mg catalyst amount. (In Au/Al₂O₃ the metal loading was 0.1 mmol/g_{cat.} while in the other samples 0.2 mmol/g_{cat.})

Table 4. Amount of CO desorbed during TPD from -20°C to 400°C, and IR band intensity of CO adsorbed on Au and Ag⁺ sites at room temperature in 1% CO in Ar flow.

Samples	CO desorbed during TPD (from -20°C to 400°C) μmol/mmol metal		IR band intensity of CO ads. on Au at RT normalized to 1wt% Au		IR band intensity of CO ads. on Ag ⁺ at RT normalized to 1wt% Ag	
	calcined	reduced	calcined	reduced	calcined	reduced
SOL Au/Al ₂ O ₃	53	29	6.6 ^x	4.8 ^x	-	-
SOL Au4Ag1/Al ₂ O ₃	38	14	6.2	4.2	0.3	0.0
SOL Ag/Al ₂ O ₃ [*]			-	-	3.6	0.3
SOL Ag/Al ₂ O ₃	66	4				
SMAD Au/Al ₂ O ₃			0.4	0.1	-	-
SMAD Au4Ag1/Al ₂ O ₃	13	1	0.0	0.0	0.0	0.0
SMAD Ag/Al ₂ O ₃			-	-	1.1	0.0

* SOL Ag/Al₂O₃^{*} contained only 1wt% Ag

^x IR was measured on SOL Au^{*}/Al₂O₃

Based on the CO adsorption and CO-TPD results it is suggested that on the surface of SOL Au4Ag1/Al₂O₃ significant amount of Au sites adsorbing CO was present in somewhat less concentration, than in corresponding Au/Al₂O₃. While on SMAD Au4Ag1/Al₂O₃ there was no such Au sites available, on the contrary that on monometallic SMAD Au/Al₂O₃ there were some, but much less than on SOL analogue. Presumably Ag in the SMAD bimetallic sample covered Au sites, but not in the SOL one. In SMAD samples the organic contaminations retained also after calcination blocked Au and Ag sites. Presence of Ag⁺ was detected by CO-TPD measurements preceded by CO adsorption at -20°C on the surface of both SOL and SMAD bimetallic Au4Ag1/Al₂O₃ samples, what was hardly or not visible, respectively, by DRIFT in CO adsorption at room temperature.

On Fig. 10 a and c the **benzyl alcohol oxidation** conversion curves of alumina and silica supported SOL samples measured with K₂CO₃ addition, and the initial reaction rates calculated from these related to 1 mg Au content are shown, respectively. There was no significant difference between alumina supported Au and Au4Ag1 activity related to the same Au content, while in case of the lower activity silica supported Au4Ag1 sample, small synergetic effect between Au and Ag was observed. However, this latter was much lower extent, than that measured in base free reaction

conditions (Fig. 10 d), where much lower initial reaction rates and fast deactivation were observed. The Au1Ag1/Al₂O₃ and Ag/Al₂O₃ catalysts had negligible activity. The reduced samples were more active than the calcined ones. The difference was very small in reaction with base addition in case of alumina supported samples, larger in case of silica supported ones, the largest in base free reaction.

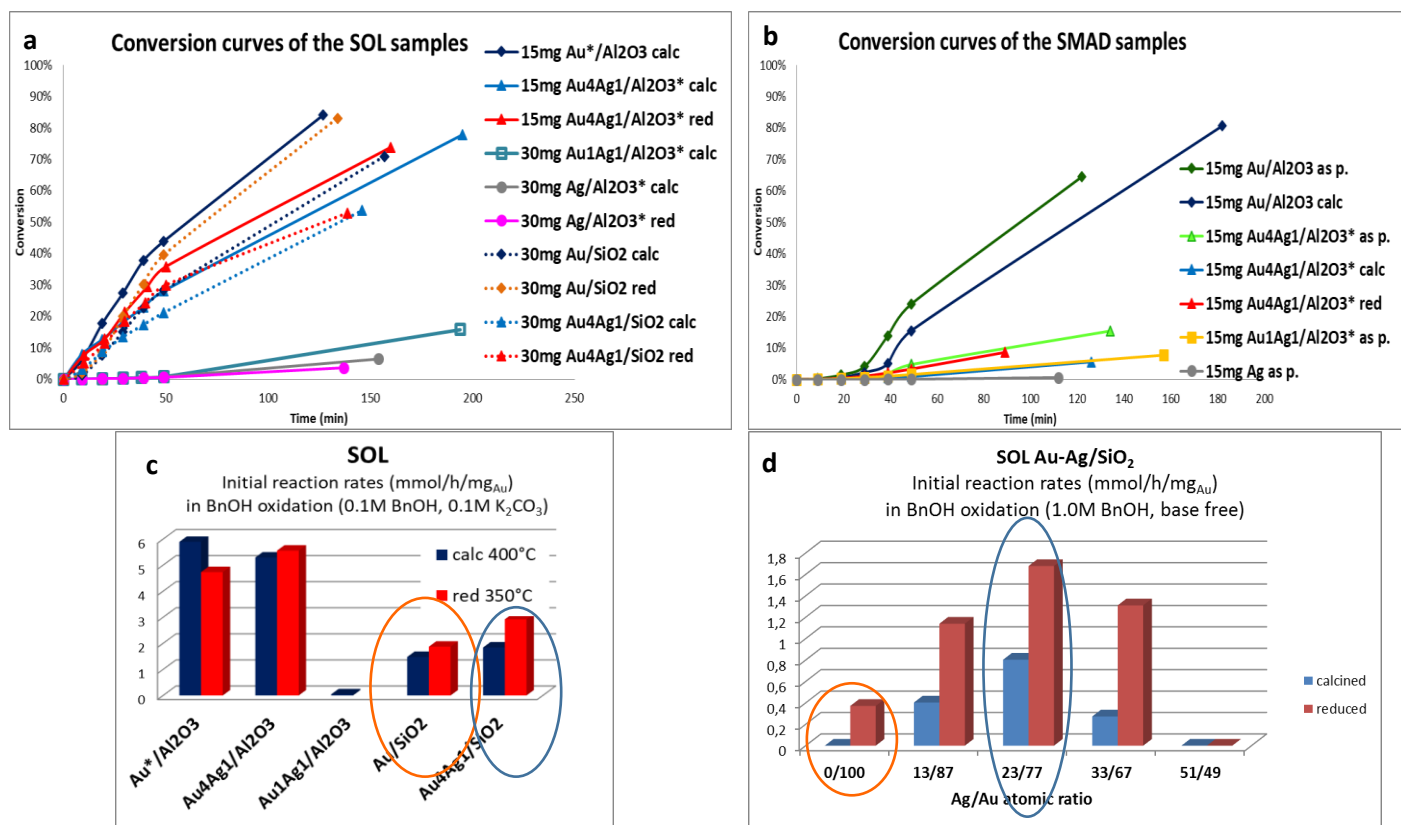


Fig. 10 Conversion curves (a, b) and initial reaction rates (c) of benzyl alcohol oxidation on the different, differently pretreated samples with base addition (30ml 0.1 M BnOH solution in toluene, 0.1M K₂CO₃, 80°C, 1 bar O₂ bubbling). For comparison initial reaction rates of silica supported catalysts in base free reaction conditions (d). (Au4Ag1/Al₂O₃*, Au1Ag1/Al₂O₃* and Ag/Al₂O₃* designate the analogues of the catalysts labelled without *, with half metal loading.)

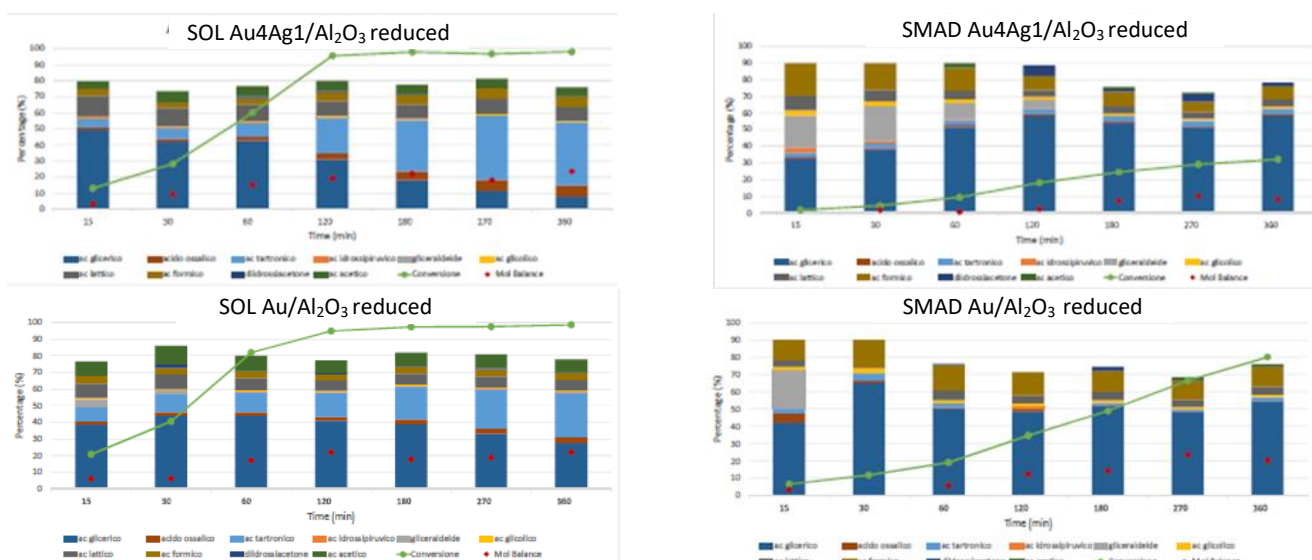


Fig. 11 Conversion of glycerol (—) and selectivity of the various products (bars) on reduced SOL and SMAD Au4Ag1/Al₂O₃ and Au/Al₂O₃ in glycerol oxidation (0.3M Gly in water, Gly/NaOH=1/4, Gly/metals=2000 mol/mol, 3 bar O₂, 50°C). Products were glyceric acid, oxalic acid, tartaric acid, hydroxypyruvic acid, glyceric aldehyde, glycolic acid, lactic acid, formic acid, dihydroxy acetone, acetic acid. Mol balance (•).

The SMAD catalysts showed an induction period in the BnOH oxidation with base addition (Fig. 10 b), after that reaction rate of the monometallic Au/Al₂O₃ was similar to that of the SOL analogue, but the bimetallic catalysts had very

low activity ($\text{Au}_4\text{Ag}_1/\text{Al}_2\text{O}_3$ somewhat higher, than $\text{Au}_1\text{Ag}_1/\text{Al}_2\text{O}_3$) and $\text{Ag}/\text{Al}_2\text{O}_3$ was inactive. The surface contamination detected by CO adsorption measurements and by XPS could be the reason of the induction period, during that in the organic media the active sites became accessible for the reactants. It is interesting, that the as prepared samples were more active than the calcined ones, maybe due to the increased metal particle size of the treated samples, while the removal of organic residues was still not complete.

The alumina supported SOL and SMAD catalysts were tested also in **glycerol oxidation**. As illustration the conversions and selectivities of the reduced SOL and SMAD $\text{Au}_4\text{Ag}_1/\text{Al}_2\text{O}_3$ and $\text{Au}/\text{Al}_2\text{O}_3$ catalysts are presented on Fig. 11. The activity of $\text{Ag}/\text{Al}_2\text{O}_3$ samples were negligible in all states studied (as prepared, calcined, reduced). The SOL catalysts were more active partly due to the smaller particle sizes, than the SMAD ones, on the other side the tartronic acid selectivity was higher on the SOL catalysts. The Ag addition did not affect significantly the activity of Au in glycerol conversion, but clearly increased the transformation of glyceric acid to tartronic acid on SOL samples, and slightly also on the SMAD ones. The bimetallic SMAD catalysts deactivated in the course of reaction, while the monometallic $\text{Au}/\text{Al}_2\text{O}_3$ not. The calcination pretreatment changed a bit the activities, differently on the various samples, and increased the tartronic acid selectivity on SOL $\text{Au}/\text{Al}_2\text{O}_3$. Surprisingly, the subsequent reduction of the calcined samples did not modify the activity nor the selectivity much.

Au-Cu bimetallic systems

Au-Cu (with molar ratio of $\text{Au}/\text{Cu}=1/1$) and the corresponding monometallic catalysts were prepared by sol deposition technique. Sols were formed using NaBH_4 reducing and PVA stabilizing agent by co- and consecutive reduction of the precursor ions ($\text{Au}\&\text{Cu}$, $\text{Au}\rightarrow\text{Cu}$: Au reduction on Cu NPs, and $\text{Cu}\rightarrow\text{Au}$: Cu reduction on Au NPs). Several samples were prepared repeatedly, which are designated by asterisk(s), as e.g. $\text{Au}\&\text{Cu}^*$, and their metal particle sizes were slightly smaller. Larger co-reduced particles and monometallic Au NPs were produced using Na-citrate stabilizing agent instead of PVA (these sols are designated by # $\text{Au}\&\text{Cu}$, #Au and #Cu). The sols were adsorbed on Degussa alumina or Aerosil silica supports. The samples prepared are listed in Table 5, with their metal loadings and mean metal particle diameters after different treatments. The mean metal particle sizes determined by TEM varied between 1.8 and 2.9 nm in the smaller size samples and 3.2 and 4.3 nm in larger size catalysts including the as prepared, calcined and reduced samples. Only the treatments at 500°C caused some significant sintering in some cases resulting in slightly larger size.

Table 5. Metal loadings and metal particle sizes in various supported bimetallic Au-Cu and corresponding monometallic catalysts

Sample	Au/Cu loading wt%	Particle diameter (nm)				
		Sol/as prep	Calcined ($400^\circ\text{C}/1\text{h}/\text{air}$)	Reduced ($350^\circ\text{C}/0.5\text{h}/\text{H}_2$)	Reduced ($500^\circ\text{C}/2\text{h}/\text{H}_2$)	Thermal treat. ($500^\circ\text{C}/2\text{h}/\text{Ar}$)
$\text{Au}/\text{Al}_2\text{O}_3$	1.80 / -	2.9 ± 1.1	2.8 ± 0.9	2.9 ± 1.1	2.8 ± 0.9	3.2 ± 0.9
$\text{Au}^*/\text{Al}_2\text{O}_3$	1.8 / -	1.9 ± 0.7	1.9 ± 0.5			
$\text{Au}^{**}/\text{Al}_2\text{O}_3$	1.8 / -	2.2 ± 0.7	1.9 ± 0.5	2.1 ± 0.5		
$\text{Au}\rightarrow\text{Cu}/\text{Al}_2\text{O}_3$	0.90 / 0.26	1.9 ± 0.5	2.6 ± 0.8	2.2 ± 0.7	2.6 ± 1.0	
$\text{Cu}\rightarrow\text{Au}/\text{Al}_2\text{O}_3$	0.89 / 0.29	2.0 ± 1.1		2.7 ± 0.9	3.5 ± 0.9	
$\text{Au}\&\text{Cu}/\text{Al}_2\text{O}_3$	0.89 / 0.30	2.5 ± 0.8	2.3 ± 0.5	2.1 ± 0.4	2.5 ± 0.5	2.6 ± 0.8
$\text{Au}\&\text{Cu}^*/\text{Al}_2\text{O}_3$	0.9/0.3		1.8 ± 0.4			
$\text{Au}\&\text{Cu}^*/\text{SiO}_2$		1.8 ± 0.4				
$\text{Au}\&\text{Cu}^{**}/\text{Al}_2\text{O}_3$	1.70/0.63	1.8 ± 0.4				
$\text{Cu}/\text{Al}_2\text{O}_3$	- / 0.60	2.8 ± 0.6				
#Cu/ Al_2O_3	- / 0.63					
#Au/ Al_2O_3	1.8/ -	3.2 ± 0.6	3.6 ± 1.0			
#Au&Cu/ Al_2O_3	0.9/0.3		4.2 ± 1.0	4.2 ± 0.9		
#Au/ SiO_2	1.7/ -	3.2 ± 0.6	3.5 ± 1.2			
#Au&Cu/ SiO_2	0.9/0.3		4.3 ± 0.9			

Different characterisation techniques were applied to investigate the interaction of gold and copper in the bimetallic samples. **Scanning transmission electron microscopy (STEM)** measurements in combination **with energy dispersive x-ray spectroscopy (EDS)** were applied to determine the arrangement and concentration of Au and Cu in single particles. On Fig. 12 illustrative Au and Cu maps (produced from the sets of EDS spectra recorded by scanning the selected area by 0.1 nm step size) of particles in the three different sols are shown with the HAADF image measured

simultaneously. The maps give a qualitative image on the distribution of the two metals that seems to be even, with no remarkable segregation of Au or Cu in any of the three type sols. However, in several cases, rather in Cu->Au sol some small excess of Cu at the rim of the particles was perceptible. The Au/Cu atomic ratio measured was much lower than the Au/Cu=1/1 bulk value, so Cu(-oxide) must be present in the sols also in separate particles.

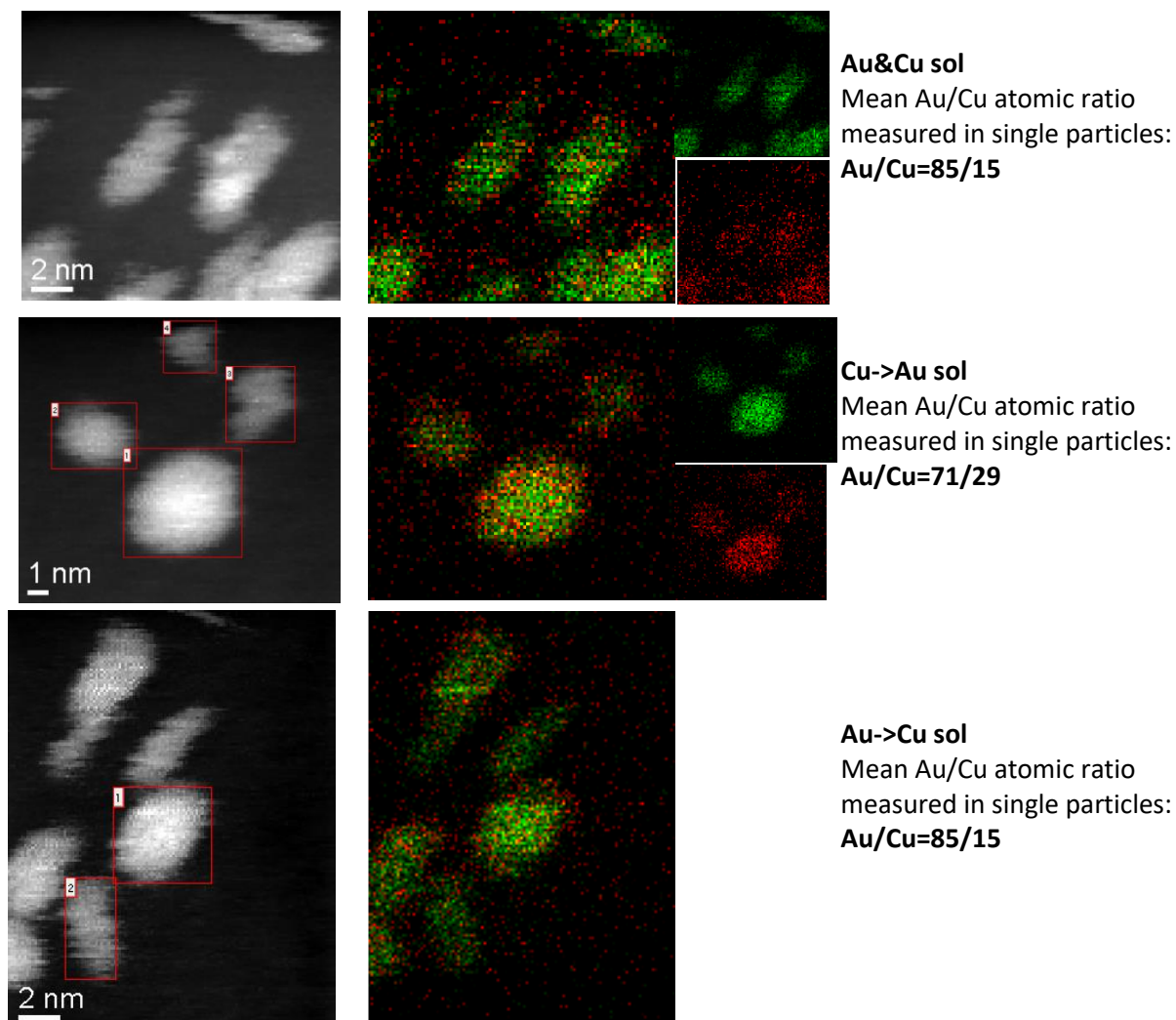


Fig. 12 Au (green) and Cu (red) maps of particles in the three different sols with the HAADF image measured simultaneously.

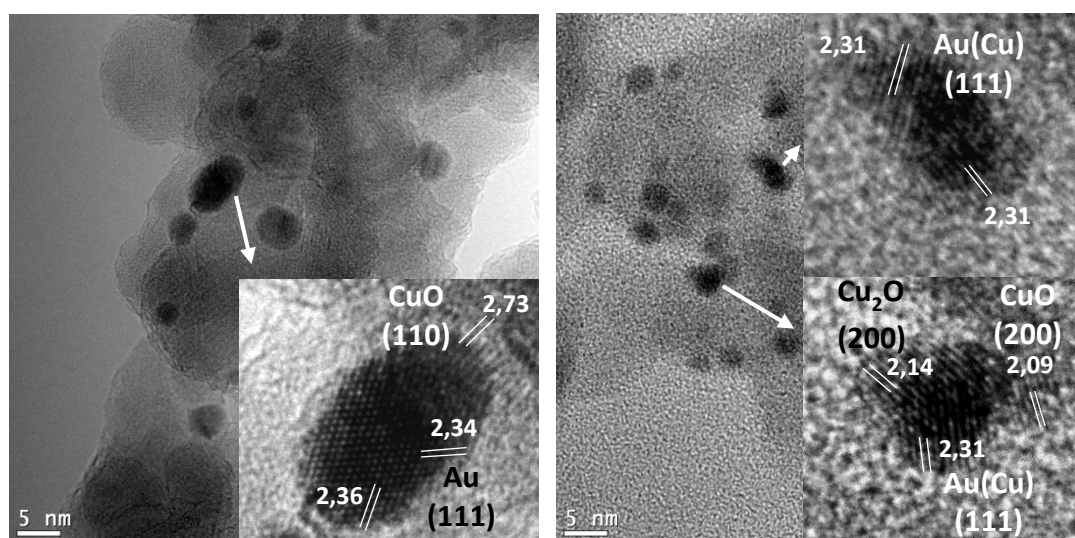


Fig. 13 HRTEM images of calcined Cu->Au/Al₂O₃ (left hand side) and Au->Cu/Al₂O₃ (right hand side)

Detailed **HRTEM investigation** were done with measurement of lattice distances in the three different alumina supported samples in as prepared, calcined and reduced state. On Fig. 13 two representative HRTEM images of calcined $\text{Cu}\rightarrow\text{Au}/\text{Al}_2\text{O}_3$ and $\text{Au}\rightarrow\text{Cu}/\text{Al}_2\text{O}_3$ can be seen, where CuO phases in connection with Au and AuCu alloyed metal phases, respectively, are visible, and also Cu_2O over the AuCu particle. Table 6 summarizes the average lattice distances determined in Au containing particles of the different samples. Taking into account the Vegard's law and that the $\text{Cu}(111)$ lattice distance is 2.09 \AA , these values showed alloyed particles in the as prepared bimetallic catalysts with lower than 20 atomic % Cu content, the highest in as prepared Au&Cu, smaller in $\text{Au}\rightarrow\text{Cu}/\text{Al}_2\text{O}_3$ and rather monometallic Au was measured in $\text{Cu}\rightarrow\text{Au}/\text{Al}_2\text{O}_3$. The calcination treatment resulted in a bit increased lattice distances, showing even lower Cu content of the alloy, and more Cu-oxide phases visible (as shown on Fig. 13). After reduction the three samples became more similar, than in as prepared state containing alloy of low, about 10-15 at. % Cu concentration.

XRD of these samples beside the intense alumina reflections showed only very weak reflections of Au(Cu) phases overlapping with the former ones, so their position could not be precisely determined, that way we could not get more information about the composition of alloyed AuCu phases. No sign of incidental monometallic $\text{Cu}(\text{O}_x)$ could be discerned.

Table 6 Mean Au(Cu) (111) lattice distance measured in the different, variously pretreated Au containing catalysts (lattice distance of $\text{Cu}(111)$ is 2.09 \AA)

Au(Cu) (111) mean lattice distance, \AA			
Sample	As prepared	Calc ($400^\circ\text{C}/1\text{h}/\text{air}$)	Red ($350^\circ\text{C}/0.5\text{h}/\text{H}_2$)
$\text{Au}/\text{Al}_2\text{O}_3$	2.34 ± 0.03		
$\text{Au}\&\text{Cu}/\text{Al}_2\text{O}_3$	2.29 ± 0.05	2.32 ± 0.03	2.30 ± 0.03
$\text{Au}\rightarrow\text{Cu}/\text{Al}_2\text{O}_3$	2.31 ± 0.03	2.32 ± 0.03	2.32 ± 0.06
$\text{Cu}\rightarrow\text{Au}/\text{Al}_2\text{O}_3$	2.34 ± 0.03	2.33 ± 0.03	2.31 ± 0.04

UV-vis spectra of sols and supported samples are presented in Fig. 14. Spectra of the bimetallic sols showed clear red shift of SPR bands related to that of monometallic Au sol. The spectra of Au&Cu and $\text{Au}\rightarrow\text{Cu}$ were almost identical with 15 nm blue shift of SPR band, while in spectrum of $\text{Cu}\rightarrow\text{Au}/\text{Al}_2\text{O}_3$ 18 nm blue shift was observed. The band shift of SPR of AuCu bimetallic colloids in linear correlation with the composition of the particles was reported in the literature. Based on the SPR band position of Au and Cu (522 and 571 cm^{-1} , respectively), and the assumed linear relation with Au molar ratio and wavelength of SPR band, maximum 30, 30, 36 atom% of Cu content of alloyed AuCu phases in Au&Cu, $\text{Au}\rightarrow\text{Cu}$ and $\text{Cu}\rightarrow\text{Au}$ sols, respectively, can be estimated, which is higher somewhat, than that calculated based on the lattice distances. Since the bulk $\text{Au}/\text{Cu}=1$, this means that the missing Cu must be present likely in separated particles or in the bimetallic particles in separated phase, rather in form of Cu-oxide because of air contact of the sols. Indeed, in the spectrum of $\text{Cu}\rightarrow\text{Au}$ sol a weak, but clear shoulder at 260 nm supposedly belonging to Cu_2O is visible. Cu_2O could be located also over the Au(Cu) particles, which might have caused a part of the blue shift of SPR band beside alloying. In the other two bimetallic sols no sign of Cu or Cu_2O can be found. In the spectra of as prepared bimetallic alumina supported samples the SPR band appeared at lower wavelength, than in the corresponding sols, while in case of monometallic Au at the same position both in sol and supported form that is not understood, yet. The monometallic $\text{Cu}/\text{Al}_2\text{O}_3$ did not present clear SPR of metallic Cu, copper must have been dominantly in oxidised state due to storing in air. The pretreatments (calcination, reduction) did not affect the spectrum of monometallic $\text{Au}/\text{Al}_2\text{O}_3$, but in case of bimetallic systems a smaller red shift of SPR band after calcination, a larger after milder temperature reduction, and even larger after stronger reduction resulting in band of 20-25 nm higher wavelength, than in case of monometallic gold sample were induced. This suggested a higher extent alloying of Cu and Au after higher temperature reduction. Indeed, in $\text{A}\&\text{Cu}/\text{Al}_2\text{O}_3$ reduced at $500^\circ\text{C}/2\text{h}$ the average atomic composition of single particles measured was $\text{Cu}/\text{Au}=25/75$, higher than the $\text{Cu}/\text{Au}=15/85$ in the corresponding sol.

^{197}Au Mössbauer measurements were carried out on as prepared $\text{Au}\&\text{Cu}/\text{Al}_2\text{O}_3$ and $\text{Cu}\rightarrow\text{Au}/\text{Al}_2\text{O}_3$ and as reference on $\text{Au}/\text{Al}_2\text{O}_3$ of eight times higher metal loadings as the normal ($0.1 \text{ mmol}/\text{g}_{\text{cat}}$) for better quality spectra. Spectra (see Fig. 15) were decomposed into a singlet and 3 doublets. The different, -1.17 , -1.00 and 0.93 mm/s isomer shifts of singlets assigned to core of the NPs for alumina supported Au, $\text{Cu}\rightarrow\text{Au}$ and Au&Cu, respectively, indicated the presence of low Cu content of AuCu alloy in bimetallic catalysts in agreement with the results of other techniques. The 2 doublets under the singlet originated from surface atoms surrounding the core of the NPs: bare and those interacting with the support. The small intensity doublet with large quadrupole splitting could be associated with an electron deficient $\text{Au}^{\delta+}$ state induced and stabilized by CuO_x formed partly on the surface of the NPs in case of the bimetallic samples, and by PVA in case of the monometallic sample.

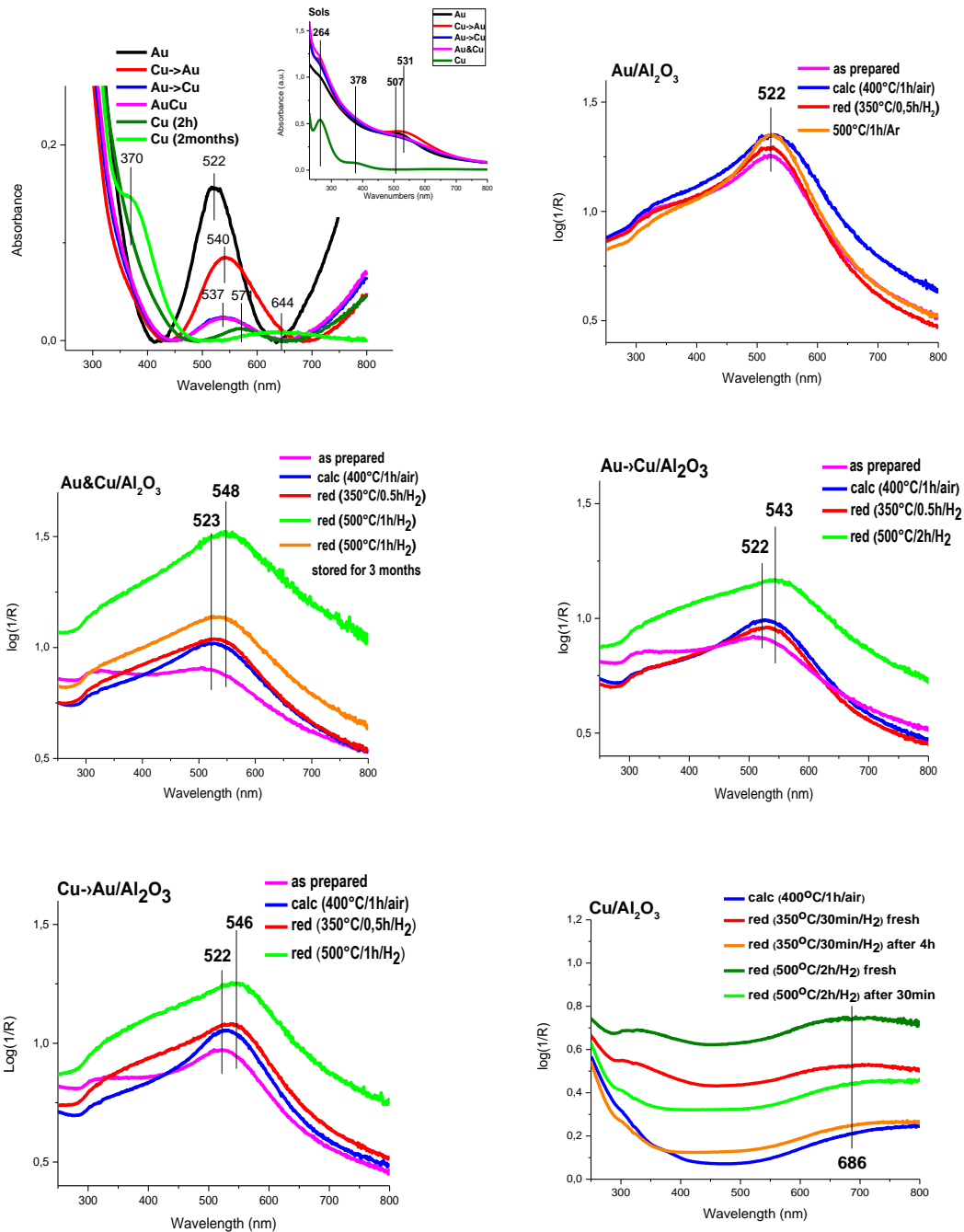


Fig. 14 UV-vis spectra of AuCu and monometallic sols and the alumina supported samples after various treatments

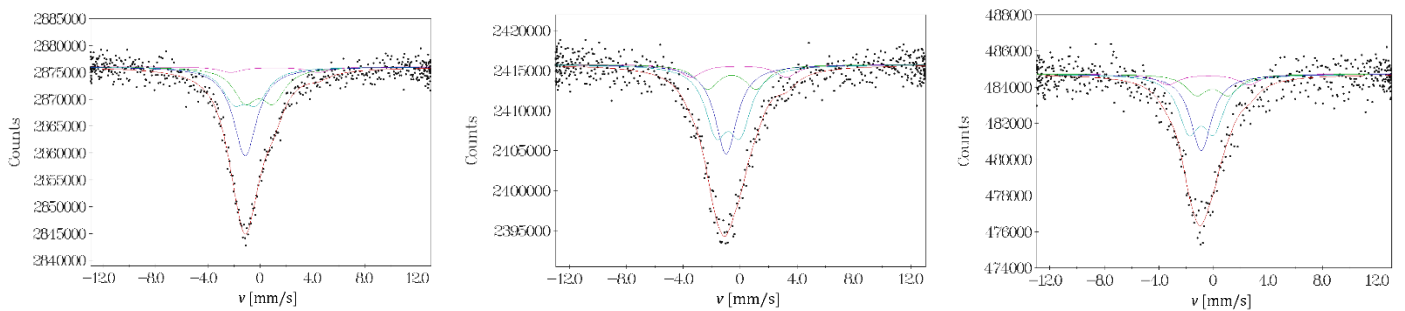


Fig. 15 ^{197}Au Mössbauer spectrum of as-prepared $\text{Au}/\text{Al}_2\text{O}_3$ (left), $\text{Cu}\rightarrow\text{Au}/\text{Al}_2\text{O}_3$ (middle) and $\text{Au}\&\text{Cu}/\text{Al}_2\text{O}_3$ (right)

XPS investigation of the 3 types of bimetallic $\text{Au-Cu}/\text{Al}_2\text{O}_3$ samples and the respective monometallic ones were carried out after different in situ pretreatments. As an illustration the Au 4f and Cu $2p_{3/2}$ XPS spectra of $\text{Au}\&\text{Cu}/\text{Al}_2\text{O}_3$ are presented on Fig. 16. The Au 4f bands for the Au-containing samples could be decomposed in two doublets, one

belonging to metallic Au⁰ and the other one to Au^{δ+}. The Cu metal and Cu⁺ (Cu₂O) is difficult to differentiate based on Cu 2p peaks especially if also CuO bands are overlapping with these. However, the shake up component at around BE: 944.5 eV characteristic of CuO can help the estimation of its surface concentration, and by that the calculation of the sum concentration of Cu⁰ and Cu¹⁺ from the Cu 2p bands. Table 7 summarizes the binding energies of the peaks, the surface compositions of Au and Cu related to Al, and the relative intensity of Au^{δ+} and Cu shake up compared to the total intensity of Au and Cu, respectively.

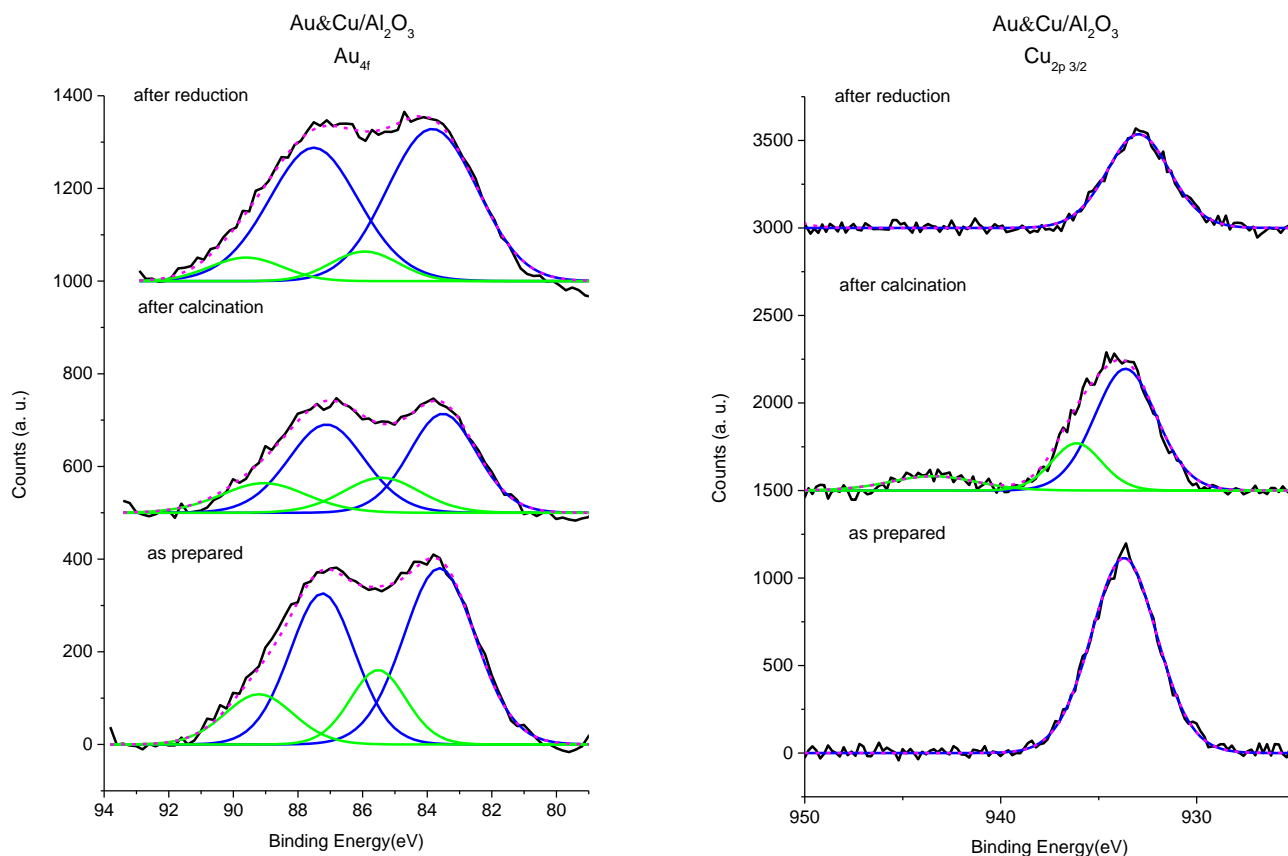


Fig. 16 XPS spectra of as prepared Au&Cu/Al₂O₃ and those recorded after consecutive in situ treatments (calcination (400°C/air/1h), reduction (350°C/H₂/30min)

The Au 4f BEs are slightly higher in the bimetallic samples, than in the monometallic one, similarly as was observed on AuAg/Al₂O₃ catalysts. However, in AuCu/Al₂O₃ also an additional doublet of 4 f_{7/2} band at about 85.5-86.5 eV appeared due to Au with partial positive charge likely as a result of interaction with Cu. The pretreatments did not change the Au 4f bands much, except in case of Au/Al₂O₃ for that in as prepared state there was a small Au^{δ+} doublet that disappeared after pretreatments, so it was suggested to belong to Au interacting with the remained PVA stabilizer. Monometallic Cu/Al₂O₃ contained in all states Cu²⁺ and also Cu⁰/Cu⁺ except after the second calcination, where negligible amount of reduced copper remained. The sum peak assigned to the Cu⁰ and Cu¹⁺ had slightly higher BEs in the monometallic sample than in the bimetallic ones. In bimetallic catalysts in as prepared and reduced state no Cu²⁺ was detected, but in calcined state the atomic ratio of Cu²⁺ in copper was about the same as in monometallic Cu. After an ex situ reduction of a calcined Au&Cu/Al₂O₃, when the catalyst was transferred quickly to the XPS spectrometer under air contact, the Cu²⁺ peaks were already there, however, with lower intensity than after in situ calcination at 400°C. It is worth to note that in monometallic Cu in the calcination-reduction-calcination treatment series the Cu/Al ratio reversibly changed, after calcination increased and after reduction decreased, similarly as Ag/Al in case of Ag/Al₂O₃, supposedly due to spreading of Cu-oxide on alumina surface and sintering of metallic Cu, respectively. In case of the bimetallic samples in the reduced form the Cu/Al ratio did not dropped as strongly as in monometallic Cu/Al₂O₃, possibly because Cu partly localised in bimetallic particles, could not be sintered in such a high extent as in Cu/Al₂O₃.

The redox properties of Cu in the bimetallic catalysts in comparison with the monometallic system was investigated by **TPR measurements** as demonstrated on Fig. 17. In the first TPR of Cu/Al₂O₃ upto 350°C with a 30min isotherm period at 350°C after the usual calcination (400°/air/1h) treatment only 75% of the theoretical H₂ uptake (calculated for CuO reduction to Cu⁰ for all copper content) was consumed. A different band structure appeared in the second TPR upto 500°C with 500°C/2h isotherm period preceded by a short calcination (400°C/5min).

Table 7. Binding energies and surface atomic ratios of Au and Cu in the different AuCu/Al₂O₃ and corresponding monometallic samples after various consecutive treatments.

Sample	B.E., eV					atomic ratio				
	Au ^{δ+}	Au ⁰	Cu ⁰ & Cu ¹⁺	Cu ²⁺	Cu ²⁺ shake up	Au ^{δ+ /} ΣAu	Au/Al %	Cu _{sat} / ΣCu	Cu/Al %	Au/Cu
Au/Al₂O₃										
as prep.	85.6	83.4				0.18	0.19			
calc.		83.1				0.00	0.13			
red. 350°C		83.2				0.00	0.13			
Cu/Al₂O₃										
as prep.			935.2	937.9	944.8			0.05	0.49	
calc.			934.8	936.4	944.6			0.14	0.67	
red. 350°C			934.1	935.7	944.7			0.10	0.16	
calc.				935.4	944.6			0.22	0.75	
Au&Cu/Al₂O₃										
as prep.	85.5	83.7	933.9			0.33	0.21	0.00	0.73	0.29
calc.	85.4	83.5	933.6	936.1	943.4	0.40	0.16	0.14	0.67	0.24
red. 350°C	85.9	83.8	933.2			0.20	0.15	0.00	0.34	0.45
ex situ red.	87.0	83.8	933.1	935.2	943.9	0.14	0.24	0.07	0.48	0.50
Cu→Au/Al₂O₃										
as prep.	85.7	83.8	934.7			0.25	0.14	0.00	0.69	0.20
calc.	85.6	83.6	934.4	936.7	944.6	0.25	0.13	0.13	0.73	0.17
red. 350°C	86.5	83.9	933.5	936.8		0.25	0.12	0.00	0.31	0.40
Au→Cu/Al₂O₃										
as prep.	85.5	83.4	934.0			0.33	0.21	0.00	0.79	0.27
calc.	85.9	83.7	934.3	936.4	944.4	0.25	0.13	0.14	0.69	0.19
red. 350°C	86.1	83.8	933.8			0.25	0.12	0.00	0.25	0.50

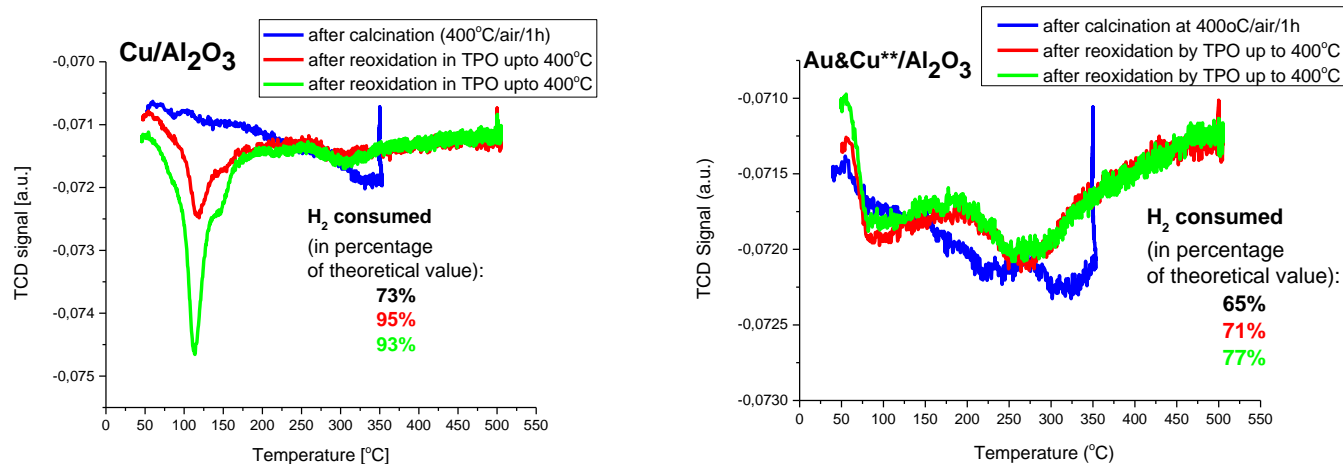


Fig. 17 TPR of Cu/Al₂O₃ and Au&Cu**/Al₂O₃ recorded in the beginning of reduction treatments preceded by oxidative treatments. (1) 350°C/10%H₂-Ar/30min after calcination (400°C/air/1h), (2) 500°C/10%H₂-Ar/2h after a short reoxidation in a TPO up to 400°C, (3) 500°C/10%H₂-Ar/5min after reoxidation in a TPO up to 400°C.

Copper of Cu/Al₂O₃ must have been fully oxidized in the reoxidation step and fully reduced in the following, second TPR, since the H₂ consumed almost reached the theoretical value. Reduction occurred at lower temperature in a sharper peak, than in the first TPR. In the first TPR the reduction of a more stable well dispersed Cu-oxide interacting with the support formed in the 1 hour calcination was supposed, while in 2nd TPR the possibly larger Cu-oxide particles formed in short reoxidation of sintered metallic Cu, with less interaction with the support resulted in lower temperature reduction peak. The third TPR again after a short reoxidation was similar to the second one, but the peak at about 125°C was even sharper. Copper easily oxidized rather to Cu₂O even at room temperature on oxygen contact (corresponding TPR is not shown). The H₂ uptake in all three consecutive TPRs (with TPOs up to 400°C in between) of the bimetallic Au&Cu**/Al₂O₃ was smaller, and the H₂ consumption band structure was more complex, than in the case of Cu/Al₂O₃. The different temperature reduction peaks indicated different Cu-oxide phases partly interacting with gold, partly

separated from gold. Metallic Cu must have been retained likely in alloy phase after calcination that explains the 25% lower H₂ uptake, than theoretical one in TPR up to 500°C. In the 2nd and 3rd TPR the lower temperature peak at around 100°C could be assigned to easily reducible Cu-oxide, likely decorating bimetallic particle surface, and the peak at around 270°C to smaller oxide particles interacting with alumina more efficiently. TPR results also supported the conclusions of other structural results, namely the presence of AuCu alloy phases with low Cu content beside Cu not interacting with gold, which readily oxidizes even at room temperature by oxygen.

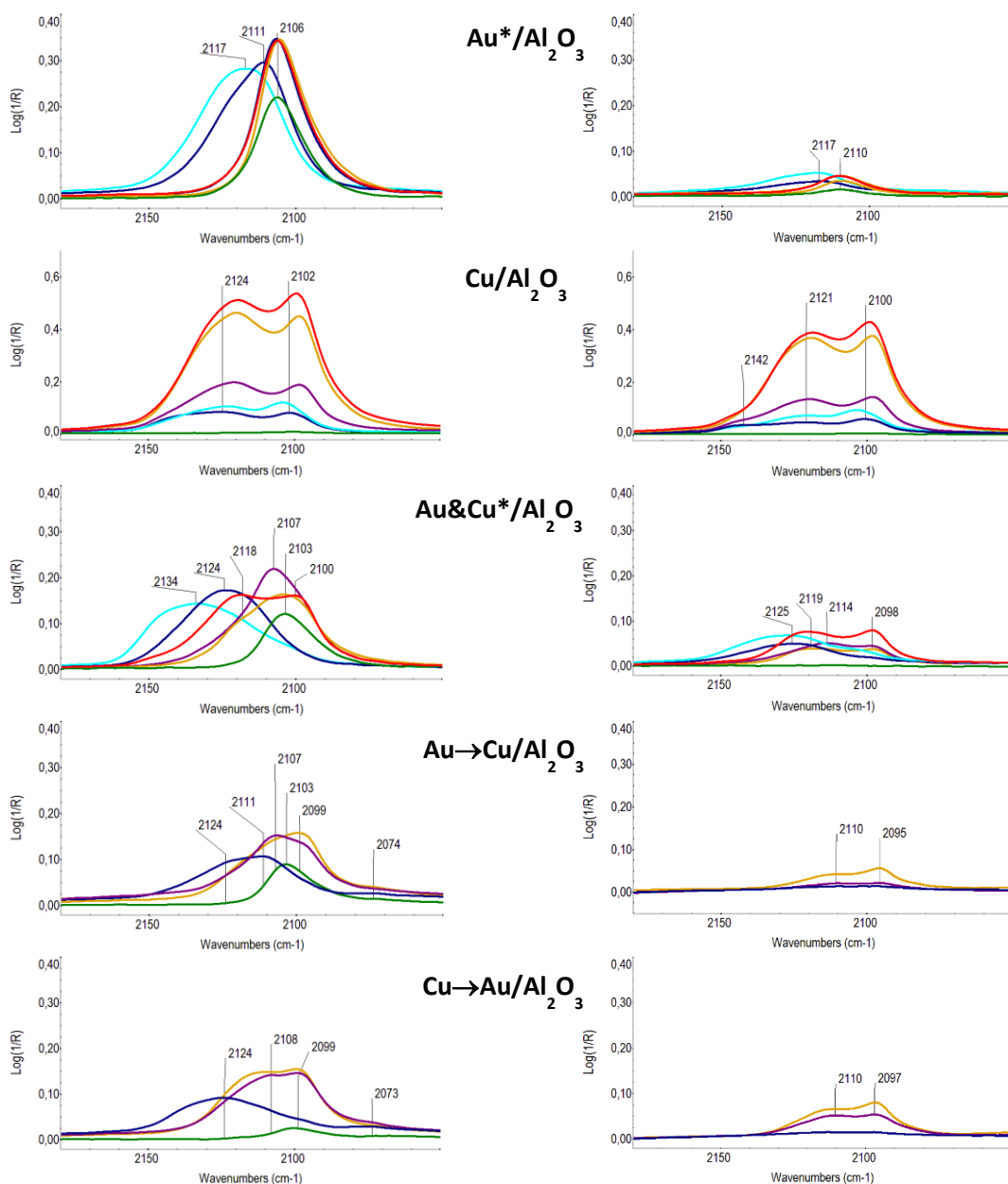


Fig. 18 DRIFT spectra of CO adsorbed in presence of 1%CO/Ar (left side, CO gas spectrum was subtracted) and after purging with Ar for 5 min (right side) on differently pretreated Au/Al₂O₃, Cu/Al₂O₃, Au&Cu/Al₂O₃, Au→Cu/Al₂O₃ and Cu→Au/Al₂O₃.

Consecutive pretreatments: (1) — ex situ calcination (400°C/air/1h), (2) — in situ 400°C/Ar/5min, (3) — in situ 400°C/air/5min, (4) — in situ 350°C/5%H₂ in Ar/40min, (5) — in situ 500°C/5%H₂ in Ar/2h, (3) — in situ 400°C/air/5min.

CO adsorption followed by DRIFT spectroscopy was investigated also on the Au-Cu/Al₂O₃ systems. A set of spectra is collected on Fig. 18. The CO adsorbed on Cu/Al₂O₃ gave the same typical band structure with different intensity after the various pretreatments, containing at least two components with similar intensity ratio, in the same spectral region, where the bands of CO adsorbed on gold appear. These bands were the weakest after calcination, much more intense on the reduced samples, and there were not large difference between the effect of milder and stronger reduction conditions. These could be assigned to Cu⁺ or Cu⁰ sites based on literature data, according to that Cu²⁺ does not adsorb CO, just Cu⁺ and Cu⁰, the former with much higher stability. In case of bimetallic samples it is difficult to distinguish the Au and Cu sites. Beside the spectra recorded in 1%CO/Ar also those measured after 5 min purging with Ar are presented,

because the bands assigned to CO adsorbed on different sites may be differentiated also by their stability. CO adsorption on copper was stronger, CO stayed longer on the surface after removal of CO gas. Among the three different bimetallic catalysts, on the Au&Cu/Al₂O₃ was estimated the largest, while on the Cu→Au/Al₂O₃ the lowest CO adsorption on Au relative to that on Cu, but significant amount Au were accessible on all three catalysts in all states. It was different in the case of Au→Ag/Al₂O₃ of the same Au/M=1/1 atomic ratio, where Au did not show CO adsorption. On the in situ calcination (with cooling in synthetic air) the blue shift of band belonging to CO adsorbed on Au^{δ+} compared to CO-Au⁰ increased on bimetallic catalysts compared to Au/Al₂O₃, similarly as on Au→Ag/Al₂O₃ indicating interaction of Au with the second metal. On the Au/Al₂O₃ treated in Ar at 400°C or reduced at different temperature CO adsorption resulted in almost identical spectra, but on the bimetallic samples the surface composition must have changed somewhat, since the spectra of CO modified.

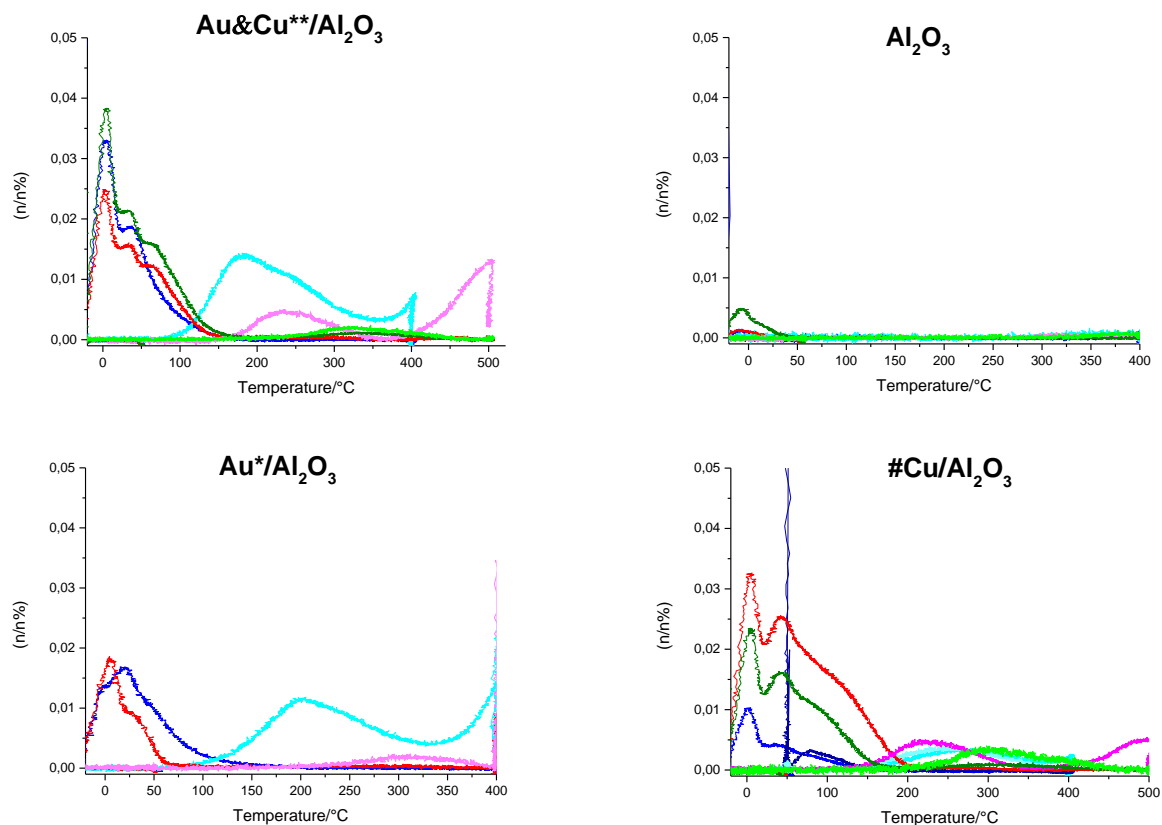


Fig. 19 TPD of CO adsorbed at -20°C (on calcined Cu/Al₂O₃ also at 50°C) on different samples calcined (400°C/10%O₂-He/1h) followed by cooling in the same gas mixture), and subsequently reduced (350°C/10%H₂-Ar/40min), then reduced again at higher temperature (500°C/10%H₂-Ar/2h). CO₂ evolution (- , - , -) during CO-TPD is also shown. The catalysts contained 0.1 mmol/g_{cat} metal, except SOL Au&Cu**/Al₂O₃ that had double metal loading (0.2 mmol/g_{cat}). The measurements were performed with 100 mg catalyst amounts.

On the **CO-TPD** curves recorded after CO adsorption at -20°C was well visible, that CO adsorbed on Cu/Al₂O₃, and also CO_{ads} on Au^{δ+} of calcined Au/Al₂O₃ desorbed completely at higher temperature, than CO_{ads} from Au⁰. From the bimetallic sample the CO_{ads} on copper left the surface at slightly lower temperature, than that from Cu/Al₂O₃. In TPD beside CO CO₂ also evolved from calcined Au/Al₂O₃ and from both calcined and reduced Au&Cu/ Al₂O₃ and Cu/Al₂O₃. This may be originated from the reaction of CO adsorbed with adsorbed oxygen or with oxygen of Cu-oxide after calcination, and with adsorbed water in case of reduced Cu-containing samples, resulting in CO₂ retained longer by alumina or Cu-oxide.

The most important **catalytic results** on the Au-Cu/Al₂O₃ are summarised on Fig. 20 and 21. In glucose oxidation the activity of gold decreased on the effect of the Cu second metal in different extent in the different type bimetallic catalysts. Among them the most active was the co-reduced Au&Cu/Al₂O₃, the Au→Cu/Al₂O₃ was less active, the Cu→Au/Al₂O₃ the least active. This was the same order as the concentration of Au sites estimated by CO adsorption decreased. It was interesting that the calcination and reduction treatment did not cause significant difference in the reaction rate. Indeed the spectra of CO adsorbed on the ex situ calcined catalysts and heated up to 400°C in Ar was hardly different from those reduced at 350°C/40min. On the other side in the bimetallic particles Cu was likely less affected in the reduction of the calcined catalysts, since it was suggested by TPR measurement, that the metallic state

of Cu was preserved during calcination due to interaction with Au in the alloy phase. Though the oxidation state of Cu separated from gold changed by reduction at 350°C of calcined samples from CuO to metallic Cu⁰ and Cu¹⁺ (according to TPR), but these could readily oxidise in air and the reaction mixture.

The alumina supported monometallic gold catalyst was about 20 times more active, than its silica supported analogue that demonstrated strong support effect, however the details and mechanism of this is unknown, yet. The AuAg/SiO₂ of Ag/Au=1/1 bulk atomic ratio was inactive in Glu oxidation, but with lower Ag/Au it became active. In the AuCu/Al₂O₃ samples, though the bulk Cu/Au was 1/1, the atomic ratio was much lower in the bimetallic particles, in that Au was accessible on the surface, while not in Au₁Ag₁/SiO₂.

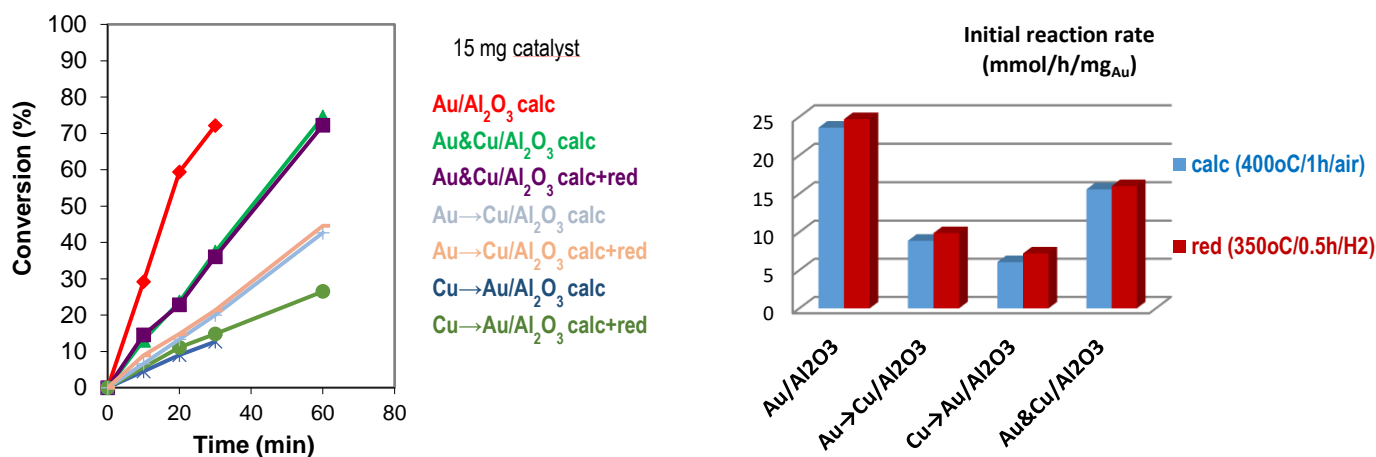


Fig. 20 Conversion curves and initial reaction rates of glucose oxidation on AuCu/Al₂O₃ catalysts and Au/Al₂O₃. Cu/Al₂O₃ was not active. (30 ml 0.1M Glu solution in water, 0.1M carbonate-bicarbonate (2:3 volume ratio) buffer, 1 bar O₂ bubbling, 35°C)

In base free benzyl alcohol oxidation the monometallic Cu/Al₂O₃ sample were not active neither in calcined nor in reduced state, while the bimetallic catalysts were more active, than the corresponding Au/Al₂O₃ of two times higher Au loading (see Fig. 21 a and b). Unfortunately, strong deactivation appeared above about 10% conversion on all the catalysts caused by benzoic acid poisoning. The difference between the 3 bimetallic catalysts were not really significant, much smaller than in glucose oxidation. The effect of mild reduction was small, while the metal particle sizes did not change drastically. In the high temperature reduction some sintering happened and the activity decreased in various extent in the bimetallic catalysts, which could not be attributed only to the decreased dispersion, but also to some rearrangement. It was interesting that after mild and high temperature reduction the activity lowered also on Au/Al₂O₃, where practically no particle size change was observed. The reason could be in water/hydroxyl concentration of the catalysts that must have been changed during the pretreatments, especially after reductions, because the reduced samples were tested just after the pretreatment, while the calcined samples only after one day, during that they could adsorb water from the ambient air. The monometallic Au/Al₂O₃ and bimetallic Au&Cu/Al₂O₃ were tested also after a treatment in inert atmosphere at 500°C/2h to reach about the same water content as after high temperature reduction, but without any redox change. Au/Al₂O₃ had the same activity after 500°C reduction and 500°C thermal treatment in inert atmosphere, but the particle size increased somewhat. After 500°C/Ar/2h treatment the activity related to one surface Au atom was lower, than after mild reduction, but higher than that after high temperature reduction. We suggest that hydrated/hydroxylated catalysts are more active, than the dehydrated ones. Au&Cu/Al₂O₃ had similar activity in calcined, mildly reduced and 500°C/Ar treated states, only reduction at 500°C lowered its activity, meanwhile the particle sizes did not differ significantly in the latter two states. In this case the surface rearrangements of the active components during treatments must also play a role, as likely in all bimetallic catalysts. However, the determination of these structural changes are challenging. Based on UV-vis measurements, up on 500°C/2h reduction an increase of Cu concentration in the alloyed phase was suggested, and in case of Au&Cu/Al₂O₃ also increased Cu/Au molar ratio in single particles was measured by HR-EDS. CO adsorption measured by DRIFT and QMS showed contradicting results on the effect of high temperature reduction. Anyway, synergistic effect lowered, but still was there on Au&Cu/Al₂O₃ and Au→Cu/Al₂O₃ after high temperature reduction. The new batch Au*/Al₂O₃ and Au&Cu*/Al₂O₃ contained smaller particles and were a bit more active, the synergy of Au and Cu was slightly lower, than in case of first batch of these samples. The mechanical mixture of Au*/Al₂O₃ and Cu/Al₂O₃ of 1/1 and also 1/2 ratio was tested as well, and increased reaction rates related to 1mg Au content was reached compared to Au*/Al₂O₃, however these were still lower than that of Au&Cu*/Al₂O₃. Thus promoting effect of copper was observed also without direct contact, interaction of Au and Cu, maybe the Cu-oxide present separately from gold might have decreased the benzoic acid poisoning effect.

The #Au&Cu/Al₂O₃ and corresponding #Au/Al₂O₃ of larger Au(Cu) particle sizes were also tested and their initial activities were smaller than those of Au&Cu*/Al₂O₃ and Au*/Al₂O₃ in calcined state, but similar synergetic effect was observed between gold and copper in this case, as well. (However, the reduced state of #Au&Cu/Al₂O₃ was much less active than expected.) The same sol derived silica supported samples (#Au&Cu/SiO₂, #Au/SiO₂) had hardly measurable activity, so strong support effect was experienced also in case of Au-Cu system, similarly as for Au-Ag system.

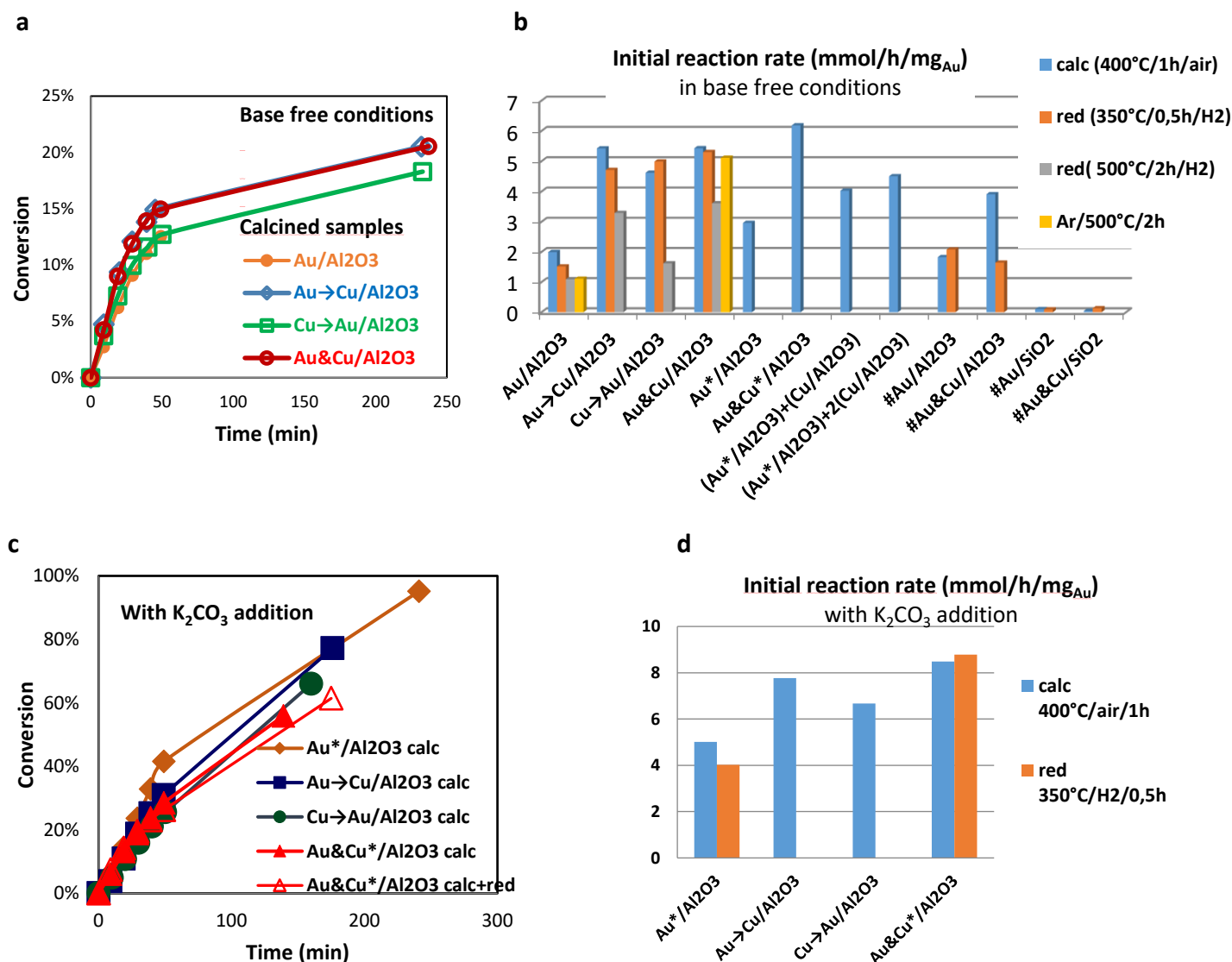


Fig. 21 Conversion curves and initial reaction rates of bimetallic alumina and silica supported Au-Cu, and monometallic Au catalysts and mechanical mixture of Au*/Al₂O₃ and Cu/Al₂O₃ in benzyl alcohol oxidation performed in base free conditions (a, b) and with base addition (c, d). Cu/Al₂O₃ was not active. (30ml 0.1 M BnOH solution in toluene, 1 bar O₂ bubbling, with/without 0.1M K₂CO₃, 80°C, 15 mg catalyst)

Benzyl alcohol oxidation was performed also with added base (equimolar K₂CO₃) by that the deactivation could be avoided. The system could tolerate about 0.5 mM benzoic acid added to the reaction mixture. The initial reaction rate of all sample increased compared to the base free reaction, because in the latter case the trace amount benzoic acid in the benzyl alcohol substrate also lowered the activity already from the beginning. The initial reaction rate of Au*/Al₂O₃ in base added reaction was about the same as that of mechanical mixture of that with Cu/Al₂O₃ in base free reaction. This suggest, that the effect of added Cu/Al₂O₃ was similar to that of K₂CO₃. In the bimetallic catalysts the synergy of Au and Cu was lower, than in base free reaction, likely because in the latter a part of this synergy originated from the protective effect of Cu-oxide separated from gold against benzoic acid, but the remaining synergy must belong to the interaction of Au and Cu(O_x) sites in the catalytic turnovers, which operates also in presence of base. The mild reduction of the calcined catalysts resulted in no important difference again, as in base free conditions.

Literature examples from the last 5-6 years showed that the combination of plasmonic gold or silver nanoparticles with wide-band gap semiconductors such as titanium dioxide and cerium dioxide can lead to an enhanced photocatalytic activity induced by irradiation in the visible range due to the strong surface plasmon resonance (SPR) excitation of such

metal NPs. Our alumina supported Au and bimetallic Au-Cu catalysts were tested in visible light irradiated photocatalytic benzyl alcohol oxidation and compared with a titania (Degussa P25) supported Au catalyst.

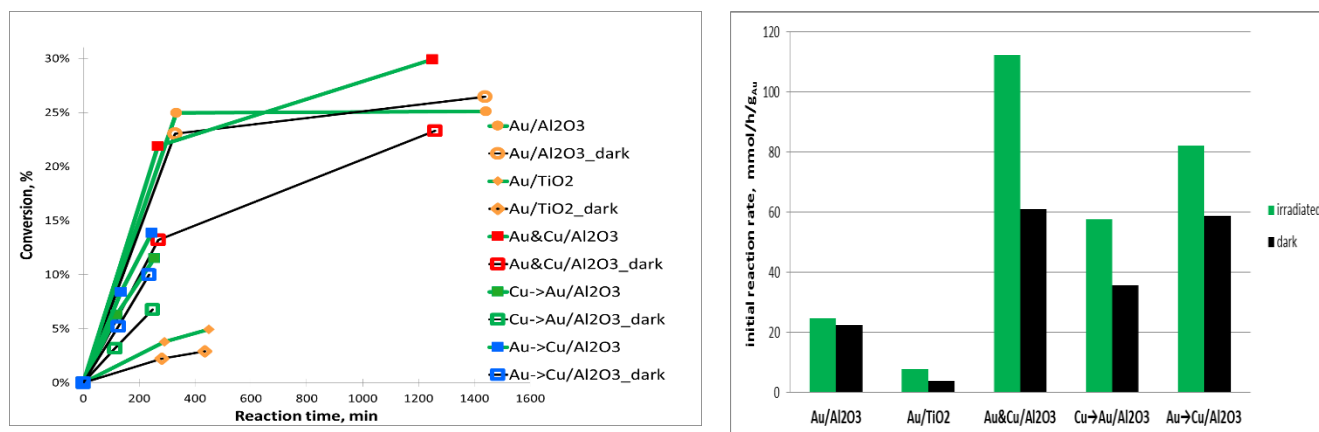


Fig. 22: Conversion curves and initial reaction rates of benzyl alcohol oxidation irradiated (530 nm) and non-irradiated (5mL 0.1 M BnOH in toluene, 1 bar O₂ bubbling, 27°C, 25 mg catalyst, in case of Au/TiO₂ 30 mg). The catalytic tests under irradiation and without irradiation were measured in two parallel experiments.

As presented in Fig. 22, all three Au-Cu/Al₂O₃ samples, like also Au/TiO₂ showed significant activity increase on the irradiation by light of 530 nm wavelength, but in case of Au/Al₂O₃ there was no difference between irradiated and non-irradiated reaction. The extent of the photo effect of the bimetallic Au-Cu/Al₂O₃ samples was slightly smaller, however, their catalytic activity was much higher, than that of the Au/TiO₂, and it depended on the structure of the bimetallic catalyst. The photo effect observed was possibly in relation with the interaction of SPR excitation of Au(Cu) and the semiconductor copper oxides.

Au-Ru and Au-Ir bimetallic systems

Alumina supported Au-Ru and Au-Ir samples of Au/M=1/1 intended atomic ratio were prepared by the same sol immobilization method, by co-reduction of precursor ions, as in case of Au&Cu/Al₂O₃. The monometallic Ru/Al₂O₃ were formed also by sol method, but the Ir/Al₂O₃ by wet impregnation technique. The Ru and especially the Ir loading of the sol derived samples were lower, than the intended ones (see Table 8). Supposedly, Ru and Ir could not be fully reduced in sol preparation and partly remained solved. The mean particle diameter in the bimetallic samples were larger, than in the monometallic ones and larger than in the analogous AuAg/Al₂O₃ and AuCu/Al₂O₃. The impregnated Ir/Al₂O₃ contained two times higher molar metal concentration than Au/Al₂O₃, but the particle size was the smallest (1.3 nm) among all the samples. The Ru and Au maps of particles in Au&Ru sol determined by scanning transmission electron microscopy (STEM) measurements in combination with energy dispersive x-ray spectroscopy (EDS) showed nicely, that Ru typically decorated the Au cores or formed shell around them. All particles measured were bimetallic, the average Au/Ru atomic ratio measured in single particles was close to the bulk value (Fig. 23).

Table 8

	Metal loading (μmol/g _{cat})		Average particle diameter (nm)	
	Au	Ru/Ir	calc (400°C/air/1h)	red (400°C/H ₂ /0.5h)
Au/Al ₂ O ₃	91		2.8±0.9	2.9±1.1
Au*/Al ₂ O ₃	91		1.9±0.5	
Au&Ru/Al ₂ O ₃	47	35	4.1±1.8	
Ru/Al ₂ O ₃		49		2.1±0.5
Au&Ir/Al ₂ O ₃	49	20	5.7±1.6	4.9±1.4
Ir/Al ₂ O ₃		193		1.3±0.8

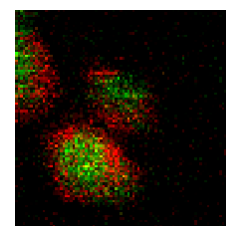


Fig. 23 Au and Ru EDS map of Au&Ru sol mean Au/Ru = 53/47

UV-vis spectra of Au&Ru sols and alumina supported samples are presented in Fig. 24. In the spectra of bimetallic sol and the as prepared Au&Ru/Al₂O₃ the SPR band typical of Au almost disappeared, a very weak, hardly visible wide band, red shifted compared to that of Au sol and Au/Al₂O₃ was observed. For an Au&Ru sol of Au/Ru=4/1 this band increased and its redshift compared to monometallic gold was smaller. (The monometallic Ru sol and as prepared Ru/Al₂O₃ had no characteristic extinction band.) This indicated an interaction between Au and Ru, an Au-core with Ru-shell character in accordance with **HR-EDS** results. After calcination of Au&Ru/Al₂O₃ SPR band similar to that of Au/Al₂O₃ (both in its frequency and intensity) appeared accompanied with an increased extinction above 600 nm that belonged

to Ru-oxide, since in calcined Ru/Al₂O₃ this feature was also visible. After reduction the bimetallic sample retained the SPR band typical of Au, the feature of calcined Ru/Al₂O₃ weakened. According to XPS results (not shown) in as prepared monometallic Ru/Al₂O₃ ruthenium was rather in RuO₂ and its smaller part in metallic state, but in the corresponding bimetallic sample the ratio of metallic Ru was larger. After calcination Ru was fully oxidised in the monometallic sample, but in the bimetallic one about 30% part was kept in metallic state. In reduction treatment at 400°C in the bimetallic sample Ru could be fully reduced, but not in monometallic one (agreeing with TPR measurements, not shown). So, in presence of gold Ru was somewhat more stable against oxidation, what also suggested the direct interaction of Au and Ru. By XRD of as prepared Au&Ru/Al₂O₃ presence of about 4 nm size metallic Au could be assumed and no Ru(-oxide) phases, but regarding the overlapping peaks with those of alumina phases, to recognise small shifts of the reflections suggesting accidental alloying was impossible. In calcined state reflections of large RuO₂ crystallites besides about 4 nm Au was clearly observed. In calcined and reduced Ru/Al₂O₃ around 30 nm RuO₂ and metallic Ru phases were estimated, but it must be kept in mind, that also small (<2-3 nm) crystallites with no visible diffraction peaks could be there.

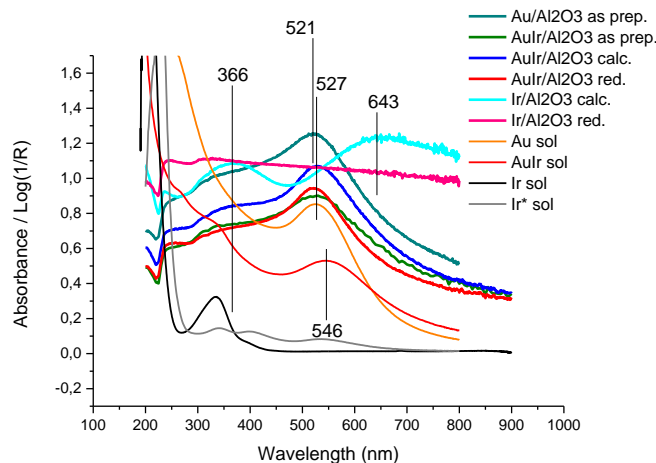
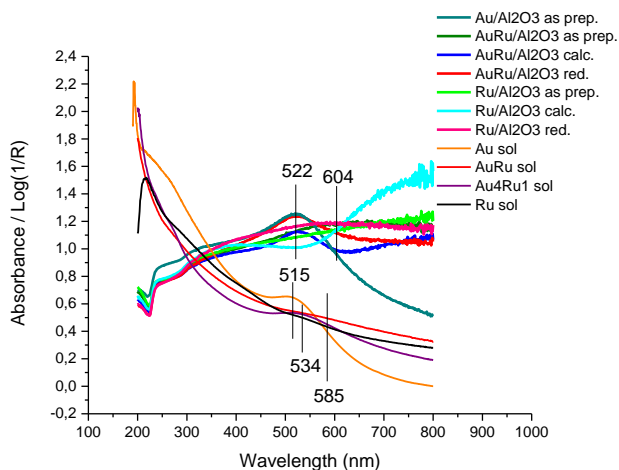


Fig. 24 UV-vis spectra of Au&Ru and monometallic sols and alumina supported samples.

Fig. 25 UV-vis spectra of Au&Ir and monometallic sols and alumina supported samples.

As can be seen on Fig. 25 the SPR band of Au&Ir sol in the UV-vis spectra was red shifted compared to that of Au sol, but this shift was hardly visible in case of the alumina supported Au&Ir related to Au. The Ir sol showed a low wavenumber band, the calcined impregnated Ir/Al₂O₃ two wide bands at 366 and 643 nm belonging to IrO₂, which disappeared after reduction. The Au&Ir/Al₂O₃ did not change much on calcination and reduction just blue shifted a tiny bit. No sign of bimetallic particles could be found in the spectra of supported samples, unless indirectly, that the features of IrO₂ could not be recognised in the spectra of calcined bimetallic sample. In the TPR of calcined Ir/Al₂O₃ and Au&Ir/Al₂O₃ the theoretical H₂ consumption (assuming total oxidation in calcination and complete reduction of iridium in the reduction treatment) were measured, however difference could be observed in the band structure of TPR curves (not presented), in the former case only one H₂ consumption peak appeared, while in the latter case two ones, one at lower and the other at higher temperature. By XRD besides Al₂O₃ reflections no Ir-containing phases could be discerned in the calcined monometallic and as prepared and calcined bimetallic samples, in the bimetallic one only about 5 nm Au with no traceable shift was supposed.

DRIFT spectra of CO adsorbed on the samples are collected in Fig. 26. Ru/Al₂O₃ showed low intensity CO bands supposedly because after calcination the large RuO₂ particles formed strongly decreased the Ru dispersion. CO bonded to Ru-sites are even more weak in Au&Ru/Al₂O₃ of lower Ru loading and containing even larger RuO₂ and likely Ru particles than Ru/Al₂O₃. CO adsorbed on Au gave about ten times lower intensity bands on the bimetallic sample, than on Au*/Al₂O₃ of double Au content and smaller particles. The CO band attributed to CO_{ads} on Au^{δ+} in calcined state is more blue shifted in case of Au&Ru/Al₂O₃ than Au/Al₂O₃ alluding some interaction with Ru(-oxide). The reduced Ir/Al₂O₃ of high and well dispersed Ir loading gave intense and band-rich spectra in the CO stretching vibration region. In calcined state it adsorbed negligible amount of CO. The reduced Au&Ir/Al₂O₃ showed CO adsorbed on Ir sites with about 5-10% intensity of that measured on Ir/Al₂O₃ of ten times higher Ir loading. The bands at 2113 cm⁻¹ was assigned surely to CO adsorbed on Au, since it desorbed quickly in purging with Ar, not as CO adsorbed on Ir, which was stable after removal of CO from the gas phase. Its intensity was not much less, than on Au&Ru/Al₂O₃. On the calcined Au&Ir/Al₂O₃ the band at 2159 cm⁻¹ belonged to Au^{δ+}, and this was even more blue shifted from that of Au/Al₂O₃ than on Au&Ru/Al₂O₃, what is a sign of Au and Ir(-oxide) interaction. The concentration of Au sites adsorbing CO in Au&Ir/Al₂O₃ was around 10% of that in Au*/Al₂O₃ estimated by DRIFT spectra of CO adsorbed and measured by CO-TPD.

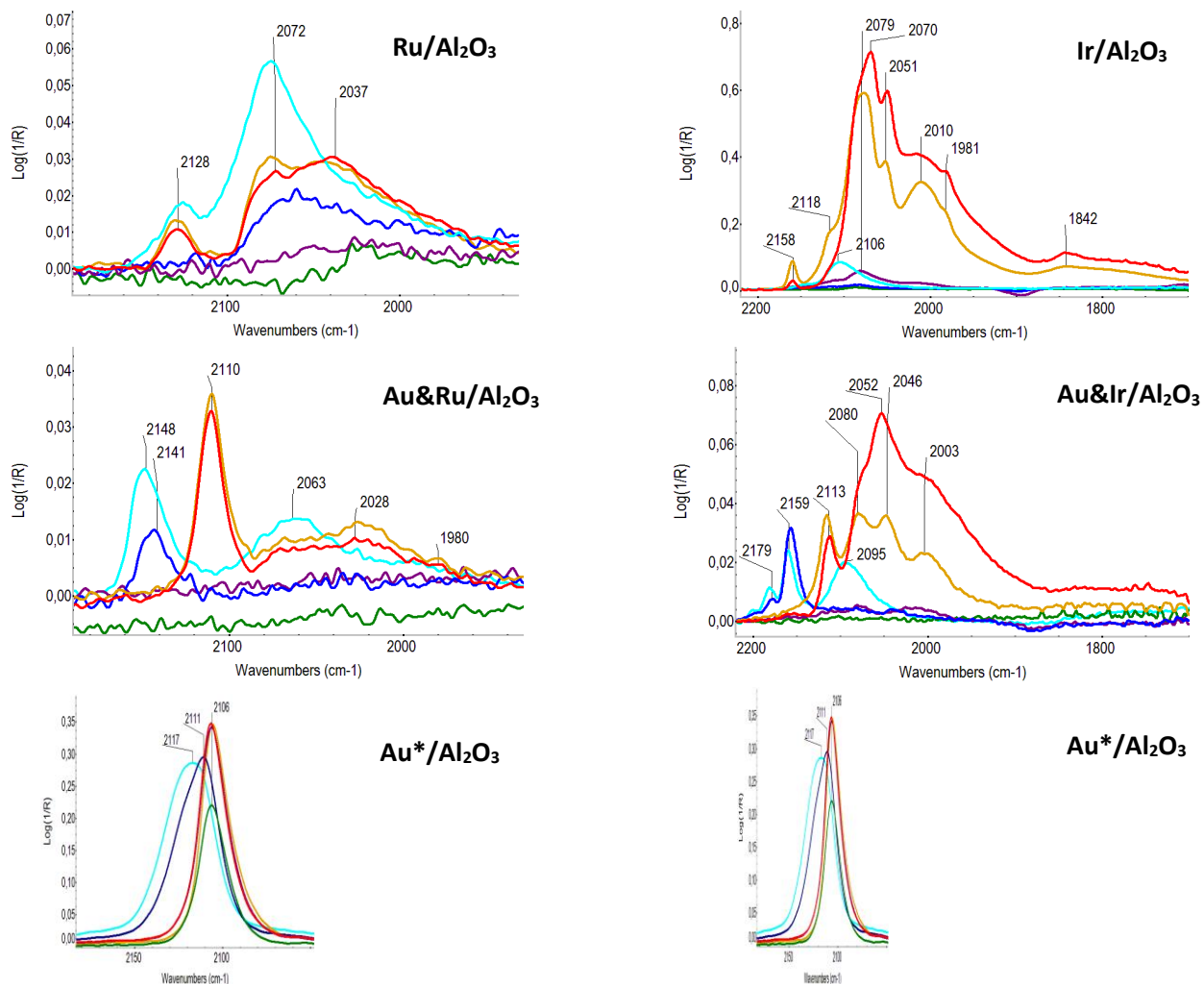


Fig. 26 CO chemisorption followed by DRIFT spectroscopy on Au&Ru/Al₂O₃ and Au&Ir/Al₂O₃ and corresponding monometallic catalysts after various consecutive in situ pretreatments: Ex situ calcination (air/400°C/1h), Ar/400°C/5min, air/400°C/5min, H₂ /400°C/30min (with cooling in Ar), H₂ /500°C/30min (with cooling in Ar), air/400°C/30min

On Fig. 27 selected glucose conversion curves and the initial reaction rates of the alumina supported Au, Au&Ru, Au&Ir and for comparison Au&Cu related to 1 mg Au content are presented. The second metal addition reduced the activity of gold. One of the reason of this was that the second metal enriched typically on the surface of bimetallic particles and reduced the accessible Au surface.

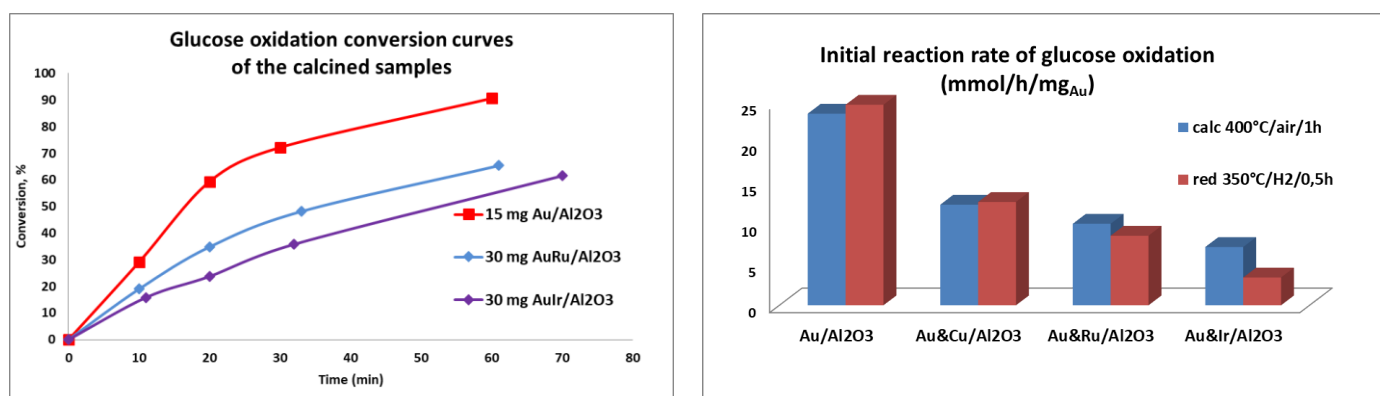


Fig. 27 Selected conversion curves and initial reaction rates related to 1mg Au of glucose oxidation reaction over alumina supported Au&Ru, Au&Ir and Au (and for comparison also Au&Cu/Al₂O₃).

Fig. 28 demonstrates the conversion curves of benzyl alcohol oxidation between base free conditions and with K₂CO₃ addition. The activity of Au&Ru/Al₂O₃ related to the same Au content was about half of that of Au/Al₂O₃ in base free conditions, both catalysts deactivated quickly. The Au&Ir/Al₂O₃ and the monometallic Ru and Ir had negligible activity. With K₂CO₃ addition the reaction on all the catalysts accelerated, the Au&Ru and Au&Ir only after an induction

period, but following that the reaction rate exceeded or almost reached that of Au/Al₂O₃, respectively. CO adsorption measurements gave an estimation on the accessible Au sites, which were about 5-10 times higher in Au/Al₂O₃, than in Au&Ru/Al₂O₃ and Au&Ir/Al₂O₃. Regarding this the active sites in the Au&Ru/Al₂O₃ and likely even in Au&Ir/Al₂O₃ probably at the interface of the two metals might be more active, than those in the Au/Al₂O₃ in glucose oxidation, but rather in benzyl alcohol oxidation. The concentration of these sites should be increased for improved catalytic performance.

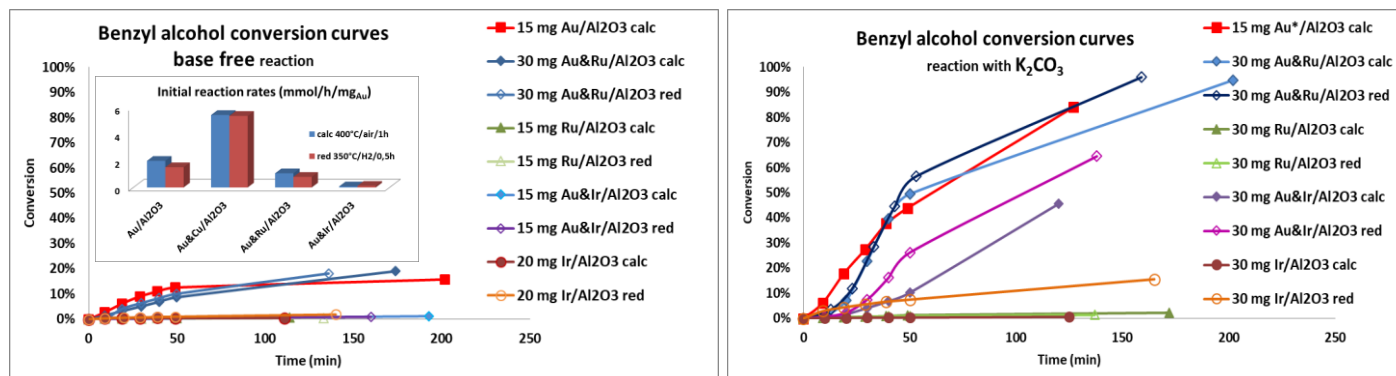


Fig. 28 Benzyl alcohol conversion curves of alumina supported Au&Ru, Au&Ir and the monometallic analogous measured in base free reaction and with K₂CO₃ addition. In the inset the initial reaction rates related to 1 mg Au in base free conditions in comparison with that of Au&Cu/Al₂O₃ are shown.

Summary

Gold-based catalysis for aerobic selective oxidation processes is an environmentally and economically viable process using O₂ as oxidant at relatively low temperature and with high selectivity for producing a wide range of useful chemicals from alcohols and carbohydrates, which are important biomass derived feedstocks. Efficiency of gold can be significantly improved or modified combining it with a second metal. Au-Ag, Au-Cu, Au-Ru, Au-Ir bimetallic systems were studied and compared in selective aerobic oxidations of model substrates, as glucose and benzyl-alcohol in the frame of our project. The effect of the second metal and the structure-catalytic effect relationship were investigated.

For studying the bimetallic effect catalysts were produced by formation and stabilization of bimetallic nanoparticles in sols or solvated metal atom dispersions (SMAD) with Au/M=1/1 intended molar ratio (in case of Au-Ag catalysts with various molar ratios, Au/Ag= 90/10, 80/10, 33/67, 50/50), followed by adsorption on alumina or silica supports. To understand the reasons of the catalytic effect of the modification of gold catalysts with a second metal detailed structural characterization was required. TEM studies showed that the size of gold containing particles were in the range of 2-3 nm in Au-Ag, Au-Cu and monometallic Au and around 4 nm in Au-Ru and 5-6 nm in Au-Ir samples, and it did not change much in the different oxidative (at 400°C) and reductive (at 350, 400 or 500°C) treatments. The presence of bimetallic particles, intimate contact of the two metals in the bimetallic catalysts were indirectly indicated by the following changes compared to the monometallic catalysts: (i) shifted SPR band of gold, (ii) modified redox properties, the higher stability of metallic state of the second metal, as characterised by TPR and XPS measurements, (iii) the modified mobility of the second metal in calcination and reduction treatments as observed by the changes of their surface concentration measured by XPS, (iv) reduced CO adsorption on gold, because of its partial covering by the second metal, (v) shifted IR bands of adsorbed CO after calcination in air at 400°C suggesting larger electron deficiency on gold in bimetallic samples. While direct confirmation of the contact of the two metals were given by HR-EDS measurement of the composition in single particles, and in case of Au-Cu HR-TEM studies showing reduced lattice distance in the metal particles and the contact of Au(Cu) particles with Cu-oxide phases. In the measured particles the Au/M ratio was close to the measured bulk ratio in the AuAg and AuRu samples, while in AuCu samples the molar Au/Cu ratio in single particles was about 85/15 instead of 1/1 bulk composition. In the AuCu/Al₂O₃ samples significant amount of copper was present separated from gold. The top surface composition of the bimetallic catalysts is decisive in the catalytic performance. The determination of that is a difficult task especially in these systems, since Au, Cu and Ag adsorbs only weakly the typical probe molecules. However, the CO adsorption measurement followed by DRIFT spectroscopy, and measured by QMS from the CO-TPD of CO adsorbed at -20°C on the different catalysts showed large differences in the concentration of Au sites adsorbing CO. The CO adsorbed on Au sites related to the same Au content decreased in the alumina supported samples in the following order (in brackets the measured bulk Au/M atomic ratio are presented): SOL Au > SOL Au-Ag (75/25) > SOL Au-Cu(50/50) >> SOL Au-Ru (60/40) ≈ Au-Ir (70/30) > SMAD Au ≈ SOL Au-Ag (Au/Ag=50/50) ≈ SMAD Au-Ag (50/50) > SMAD Au-Ag (80/20). The CO adsorption does not probe all surface Au atoms, just the ones with low coordination number, and its concentration is not necessarily proportional with that of all surface Au atoms. In case of spherical particles it depends typically on the particle size. However, in the studied systems, the mean particle sizes varied in relatively narrow range (2-5 nm), thus we can use the amount of CO adsorbed for comparing the accessible Au

surface in the different catalysts.

In all three catalytic reactions studied the Ag, Cu, Ru, and Ir monometallic analogous of corresponding bimetallic catalysts had negligible activity in the applied reaction conditions. For the catalytic turn overs Au sites must have been available that could be modified by the second metal, likely forming bimetallic active sites favouring the activation of oxygen. The activity of the bimetallic catalysts and the monometallic gold catalysts were compared by the initial reaction rate related to 1 mg gold content. The selectivity of glucose and benzyl alcohol oxidations did not vary much in the different samples, in the former reaction the gluconic acid selectivity was 100%, in the latter the benzaldehyde selectivity was above 88% beside benzyl benzoate as the only side product detected on all studied catalysts. In glycerol oxidation many products formed, their selectivity were modified on Au-Ag/Al₂O₃ related to Au/Al₂O₃.

In glucose oxidation the Cu, Ru and Ir second metal decreased (with increasing extent in this order) the activity of alumina supported monometallic Au related to the same Au content. However, if the Au surface area decrease in the bimetallic catalysts compared to the monometallic gold estimated by CO adsorption measurements is taken into account, the reaction rate related to one surface Au atoms were significantly higher in Au-Ru/Al₂O₃, and possibly in lower extent also in Au-Ir/Al₂O₃ than in Au/Al₂O₃. We cannot state this in case of Au-Cu/Al₂O₃. Though the CO adsorption of Au-Cu/Al₂O₃ systems was not much higher, than that of Au/Al₂O₃ containing the same amount of Au, but since CO adsorbed on gold and copper atoms could not be well distinguished, we could not estimate the extent of Au surface area decrease. The effect of Ag as second metal on Au was investigated in silica supported systems. If Au/Ag molar ratio was 1/1 the catalysts had no activity, because Ag covered the Au surface practically completely. Increasing the Au/Ag ratio clear synergetic activity increase was observed, the largest at Au/Ag=4/1 atomic ratio. Supposedly at this bulk composition was the highest the concentration of the most active surface sites containing Au and Ag surface atoms in optimal ratio for activation of both glucose and oxygen.

In benzyl alcohol oxidation the alumina supported bimetallic systems with all four second metals were investigated. The reaction was carried out both in base free conditions and with equimolar K₂CO₃ added. In the former case all the catalysts deactivated quickly due to the poisoning by the trace amount of benzoic acid side product. (The benzoic acid contamination of the initial benzyl alcohol in trace concentration also lowered the activity, so for comparisons the measurements with the same starting benzyl alcohol could be used only.) In case of Au-Cu/Al₂O₃ catalysts more than two times higher initial activity related to the same Au content were observed in all four differently prepared catalysts of Au/Cu=1/1 atomic ratio, while the accessible Au surface was surely not larger as compared to the monometallic Au analogue. The mechanical mixtures of the Au/Al₂O₃ and Cu/Al₂O₃ of Au/Cu=1/1 and 1/2 atomic ratio (where Au and Cu(-oxide) were present in separate particles) also presented higher initial activity, than Au/Al₂O₃, however in lower extent than in the Au-Cu/Al₂O₃. The initial activity of Au-Ru/Al₂O₃ related to 1 mg Au content was only about 50% of that of Au/Al₂O₃, but since the accessible Au surface assessed in this sample was about 10-20% of that in Au/Al₂O₃ the synergetic cooperation of Au and Ru was suggested, that was clearly confirmed for Au and Cu. Au-Ir/Al₂O₃ showed negligible activity in these conditions. With base addition the poisoning by benzoic acid could be eliminated and higher specific reaction rates could be measured. In such conditions the synergetic effect of Au-Cu/Al₂O₃ was somewhat lower, than in base free reaction. Supposedly, in the latter case it originated partly from the effect of separate Cu-oxide on the surface lowering the benzoic acid poisoning of the active sites, which did not play a role in reaction with base addition, and only partly from the direct cooperation of gold and copper in the catalytic turnovers. In presence of K₂CO₃ on Au-Ru/Al₂O₃ and Au-Ir/Al₂O₃ an induction period was observed after that the reaction rates were much increased compared to those measured without base, and surpassed or approached that of Au/Al₂O₃, respectively. Thus, taking into account the surface Au atom concentrations, large synergetic effect were suggested in these cases, larger for Au-Ru and lower for Au-Ir. The Au-Ag/Al₂O₃ of Au/Ag=1/1 had no activity, because Au was almost completely covered by Ag, while activity related to the same Au content of the Au-Ag/Al₂O₃ of Au/Ag=4/1 and Au/Al₂O₃ was about the same, and not large difference was observed in the amount of CO adsorption on Au sizing up the Au surface. Thus, the smallest synergy was suggested in this case among the studied bimetallic combinations.

In benzyl alcohol oxidation in the case of Au-Ag and Au-Cu systems also silica supported analogous were studied. In base free reaction large synergetic effect of Au and Ag was obtained on Au-Ag/SiO₂ at Au/Ag: 90/10, 80/20 and 67/33 bulk atomic ratio, while in presence of K₂CO₃ the activity increased accompanied by strong weakening of the synergy. However, in the latter conditions the activities of the corresponding alumina supported catalysts were more than two times higher with even lower synergy between Au and Ag. In base free conditions also the Au-Cu/SiO₂ and Au/SiO₂ were much less active, than the corresponding alumina supported analogues, showing hardly any conversion.

In glycerol oxidation the sol and SMAD derived alumina supported Au-Ag catalysts of Au/Ag=4/1 atomic ratio were tested. The SMAD samples were much less active than the SOL ones. In the rate of glycerol conversion the Ag introduction did not cause much effect in case of SOL samples, but clearly increased the transformation of glyceric acid to tartronic acid, and slightly also on the SMAD ones.

Large part of the results described above has not been published, yet, but most of them were presented on conferences. The preparation of further publications are in progress.

References

- 1 C. Della Pina, E. Falletta, L. Prati and M. Rossi, *Chem. Soc. Rev.*, 2008, **37**, 2077.
- 2 C. D. Pina, E. Falletta and M. Rossi, *Chem. Soc. Rev.*, 2011, **41**, 350–369.
- 3 T. Mallat and A. Baiker, *Annu. Rev. Chem. Biomol. Eng.*, 2012, **3**, 11–28.
- 4 C.-W. Yen, M.-L. Lin, A. Wang, S.-A. Chen, J.-M. Chen and C.-Y. Mou, *J. Phys. Chem. C*, 2009, **113**, 17831–17839.
- 5 N. K. Chaki, H. Tsunoyama, Y. Negishi, H. Sakurai and T. Tsukuda, *J. Phys. Chem. C*, 2007, **111**, 4885–4888.
- 6 C. Della Pina, E. Falletta and M. Rossi, *J. Catal.*, 2008, **260**, 384–386.
- 7 T. Benkó, A. Beck, K. Frey, D. F. Srankó, O. Geszti, G. Sáfrán, B. Maróti and Z. Schay, *Appl. Catal. Gen.*, 2014, **479**, 103–111.
- 8 G. Nagy, T. Benkó, L. Borkó, T. Csay, A. Horváth, K. Frey and A. Beck, *React. Kinet. Mech. Catal.*, 2015, **115**, 45–65.